Article

Cell Reports

Corrination of a GLP-1 Receptor Agonist for Glycemic Control without Emesis

Graphical Abstract

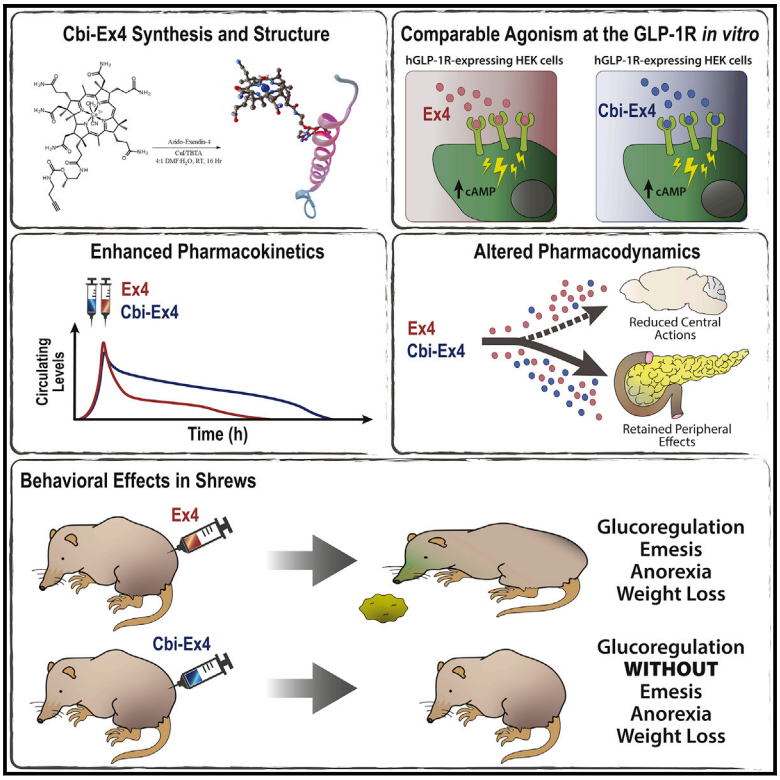

Highlights

- The Cbi-Ex4 conjugate retains GLP-1R agonism *in vitro* and improved half-life *in vivo*
- Cbi-Ex4 displays similar glucoregulatory properties compared to native Ex4
- Cbi-Ex4 does not induces anorexia, weight loss, or hindbrain neuronal activation
- In contrast to Ex4, Cbi-Ex4 does not cause emesis indicative of improved tolerance

Authors

Tito Borner, Jayme L. Workinger, Ian C. Tinsley, ..., Bart C. De Jonghe, Matthew R. Hayes, Robert P. Doyle

Correspondence

rpdoyle@syr.edu

In Brief

Borner et al. describe the creation of a conjugated GLP-1R agonist (Cbi-Ex4) with reduced brain penetrance. Cbi-Ex4 enhances glycemic control without inducing emesis or anorexia. Our preclinical findings highlight its potential therapeutic use for patients seeking improved glycemic control without the loss of appetite and emesis characteristic of current GLP-1 therapeutics.

Borner et al., 2020, Cell Reports *31*, 107768
June 16, 2020
https://doi.org/10.1016/j.celrep.2020.107768

CellPress

Cell Reports

CellPress
OPEN ACCESS

Article

Corrination of a GLP-1 Receptor Agonist for Glycemic Control without Emesis

Tito Borner,[3,7] Jayme L. Workinger,[1,7] Ian C. Tinsley,[1,7] Samantha M. Fortin,[2] Lauren M. Stein,[2] Oleg G. Chepurny,[4] George G. Holz,[4] Aleksandra J. Wierzba,[5] Dorota Gryko,[5] Ebba Nexø,[6] Evan D. Shaulson,[3] Ankur Bamezai,[2] Valentina A. Rodriguez Da Silva,[2,3] Bart C. De Jonghe,[3,8] Matthew R. Hayes,[2,3,8] and Robert P. Doyle[1,4,8,9,*]

[1]Department of Chemistry, Syracuse University, Syracuse, NY, USA
[2]Department of Psychiatry, Perelman School of Medicine, University of Pennsylvania, Philadelphia, PA, USA
[3]Department of Biobehavioral Health Sciences, School of Nursing, University of Pennsylvania, Philadelphia, PA 19104, USA
[4]Department of Medicine, Upstate Medical University, State University of New York, Syracuse, NY, USA
[5]Institute of Organic Chemistry, Polish Academy of Sciences, Warsaw, Poland
[6]Department of Clinical Biochemistry and Clinical Medicine, University of Aarhus, Aarhus, Denmark
[7]These authors contributed equally
[8]These authors contributed equally
[9]Lead Contact
*Correspondence: rpdoyle@syr.edu
https://doi.org/10.1016/j.celrep.2020.107768

SUMMARY

Glucagon-like peptide-1 receptor (GLP-1R) agonists used to treat type 2 diabetes mellitus often produce nausea, vomiting, and in some patients, undesired anorexia. Notably, these behavioral effects are caused by direct central GLP-1R activation. Herein, we describe the creation of a GLP-1R agonist conjugate with modified brain penetrance that enhances GLP-1R-mediated glycemic control without inducing vomiting. Covalent attachment of the GLP-1R agonist exendin-4 (Ex4) to dicyanocobinamide (Cbi), a corrin ring containing precursor of vitamin B12, produces a "corrinated" Ex4 construct (Cbi-Ex4). Data collected in the musk shrew (*Suncus murinus*), an emetic mammal, reveal beneficial effects of Cbi-Ex4 relative to Ex4, as evidenced by improvements in glycemic responses in glucose tolerance tests and a profound reduction of emetic events. Our findings highlight the potential for clinical use of Cbi-Ex4 for millions of patients seeking improved glycemic control without common side effects (e.g., emesis) characteristic of current GLP-1 therapeutics.

INTRODUCTION

Type 2 diabetes mellitus (T2DM) management involves lifelong pharmaceutical interventions (Drucker et al., 2011; Sadry and Drucker, 2013), including those based on glucagon-like peptide-1 (GLP-1), an incretin hormone produced in the intestine and brainstem (Hayes et al., 2014; Holst, 2007). Existing US Food and Drug Administration (FDA)-approved GLP-1 receptor (GLP-1R) agonists enhance postprandial insulin secretion and reduce food intake (Hayes et al., 2014; Hayes and Schmidt, 2016; Kanoski et al., 2016). While the latter is attractive when considering GLP-1R agonists for obesity treatment, the hypophagic effects of *all* known GLP-1R agonists are accompanied by nausea and vomiting, which affects ~20%–50% of patients and leads to discontinuation of drug treatment in ~6%–10% and reduced dose tolerance in another ~15% of patients (Bergenstal et al., 2010; Buse et al., 2004; DeFronzo et al., 2005; John et al., 2007; Kendall et al., 2005). Evidence-based medical reports are now clear that nausea and emesis are the principal side effects of existing GLP-1 therapeutics (Bettge et al., 2017). Even with common approaches to mitigate side effects such as slow-dose escalation or titration, a recent report from GlaxoSmithKline concluded that patients reported GI-related issues that "made me feel sick" (64.4%) and "made me throw up" (45.4%) as their major reasons for treatment discontinuation (Sikirica et al., 2017). Importantly, such adverse gastrointestinal events of GLP-1R agonists are persistent in the profile of current second-generation GLP-1R-based drugs such as dulaglutide, semaglutide, and albiglutide (Ahrén et al., 2018; Pratley et al., 2018; Wysham et al., 2014). Importantly, for some diabetic patients with comorbidities such as cancer, cystic fibrosis, HIV, or general disease-cachexia, *any* further weight loss and malaise are unacceptable side effects that necessitate the creation of a new class of GLP-1 therapeutic.

There is convincing evidence that a significant portion of the increase in glucose-stimulated insulin secretion following administration of current exogenous GLP-1R ligands is mediated by direct activation of GLP-1R expressed on pancreatic β-cells (for review, see Drucker, 2006; Hayes et al., 2010, 2014; Kanoski et al., 2016), mimicking the paracrine effects of pancreatic-derived GLP-1 that may not occur with endogenous L-cell-derived GLP-1(Chambers et al., 2017; Lamont et al., 2012; Smith et al., 2014). In contrast, GLP-1Rs expressed in the central nervous system (CNS), in particular those in the hindbrain (Alhadeff et al., 2016; Hayes et al., 2011), mediate the food intake- and body weight-suppressive effects of GLP-1R agonists, such as

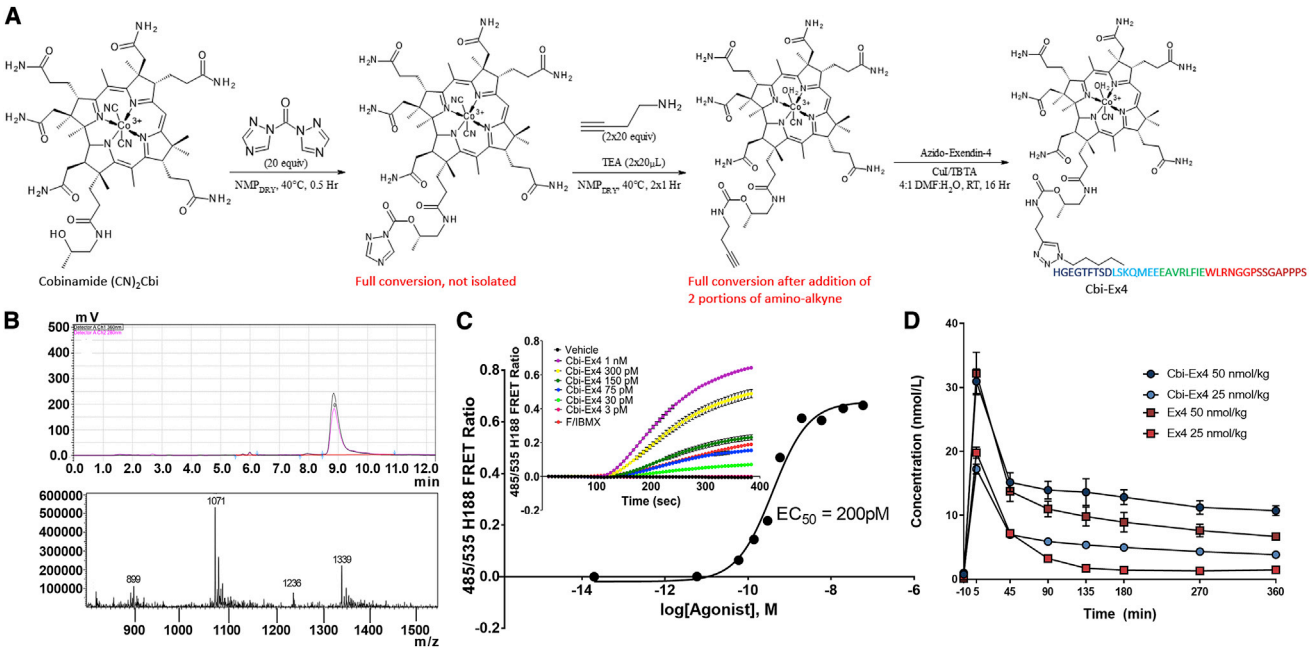

Figure 1. Covalent Conjugation of Ex4 to Cbi Retains GLP-1R Agonism *In Vitro* and Displays Improved Half-Life *In Vivo*

(A) Synthetic scheme for Cbi-Ex4 synthesis: 1-amino-3-butyne was coupled to Cbi utilizing carbonyl ditriazole (CDT), priming the Cbi for conjugation to Ex4. Ex4 was covalently bound to the Cbi-alkyne via copper-catalyzed alkyne-azide cycloaddition.

(B) RP-HPLC of Cbi-Ex4 showing purity of ≥ 97% and liquid chromatography-mass spectrometry (LC-MS) showing 1,339 $[M+4H]^{4+}$ and 1,071 $[M+5H]^{5+}$, consistent with the conjugate.

(C) Dose-dependent Cbi-Ex4 agonism at the human GLP-1 receptor, as monitored in FRET assays using the cAMP biosensor H188 expressed in HEK293 cells. EC_{50} value for Cbi-Ex4 was determined to be 200 ± 0.09 pM (mean ± SEM) (Chepurny et al., 2019).

(D) Pharmacokinetic profile of two equimolar doses (25 nmol/kg and 50 nmol/kg) of Ex4 and Cbi-Ex4. Data expressed as mean ± SEM.

Full PK parameters are given in Table S2.

liraglutide and exenatide (synthetic Ex4) (Kanoski et al., 2011; Mietlicki-Baase et al., 2013; Secher et al., 2014; Sisley et al., 2014). This CNS site-of-action, and not a vagally mediated effect, is also responsible for mediating the illness-like behaviors (e.g., nausea, conditioned taste avoidance, emesis) of systemically delivered GLP-1R agonists (Kanoski et al., 2012). Thus, from a therapeutic standpoint aimed at normalizing the chronic hyperglycemia of diabetic patients, designing a GLP-1R agonist that does not penetrate readily into the CNS (or at least the hindbrain), but retains enhanced pharmacological action on β-cells, would theoretically provide an improved tool for glycemic control without eliciting unwanted nausea/malaise.

Taking advantage of the highly controlled transport and trafficking of vitamin B12 (B12) that occurs in mammalian physiology, together with bioconjugate technology involving peptide-based conjugation to B12 and B12 fragments, Ex4 was covalently attached to dicyanocobinamide (Cbi), a corrin-ring-containing precursor of B12, to create the compound Cbi-Ex4 (Figure 1A). The theoretical advantage of this construct was 3-fold. First, there is no known biological function of Cbi in humans and Cbi does not affect intact B12 physiology (Green et al., 2017). Second, Cbi is highly water soluble and the uptake of Cbi-Ex4 through the blood brain barrier and into the CNS would putatively be extremely low (Green et al., 2017). Indeed, evidence collected postmortem from human brain and liver clearly demonstrated negligible amounts of B12 (11.3 pmol/g) and an ~10-fold lower relative concentration of corrinoid-type analogs (1.3 pmol/g; including cobinamide) in the brain, with the liver being the main site of concentration for both B12 and corrinoid analogs (total >600 pmol/g) (Kanazawa and Herbert, 1983). These first two advantages of Cbi-Ex4 provide support for the third and most important hypothesized benefit—namely that Cbi-Ex4 should theoretically be a GLP-1R agonist that retains a peripheral site of action when systemically administered, providing a pancreatic-mediated mechanism for Cbi-Ex4 to improve hyperglycemia, without producing any CNS-mediated illness-like behaviors.

Cbi has been identified in humans (Hardlei and Nexo, 2009), but has no influence on normal B12 homeostasis (Green et al., 2017) since it is *not* recognized by the B12 blood transporting protein transcobalamin (TC), critical for blood-brain barrier penetrance and cell entry via the CD320 receptor (Green et al., 2017). Instead, Cbi is recognized in blood *only* by the B12 binding protein haptocorrin (HC). The function of circulating HC is unknown and no known specific receptor for the Cbi-HC complex has been identified (Furger et al., 2012). Indeed, congenital defects in plasma HC are asymptomatic, suggesting that HC and Cbi are not physiologically relevant in humans (Rosenblatt et al., 2001). Further, the plasma-binding capacity of HC for molecular forms of B12, including Cbi, in humans is very limited (reference

interval 90–270 pM; Gimsing and Nexø, 1989). Thus, using Cbi (in a conjugate process we coin here "corination") as a pharmacodynamic/pharmacokinetic modifier of a target peptide pharmaceutical, we have created an "inert" carrier in terms of affecting B12 homeostasis, but one that would have the advantage of putatively reducing/avoiding CNS permeability/localization while improving the general proteolytic survival and/or reduce clearance of the bound peptide. Unfortunately, rodents do not represent ideal models to test Cbi-Ex4 as (1) they lack the separate HC and TC proteins as found in human blood (Kuda-Wedagedara et al., 2017) and (2) they lack the emetic reflex (Horn et al., 2013). The musk shrew (*Suncus murinus*) was therefore chosen as the model system to evaluate the *in vivo* efficacy and tolerability of Cbi-Ex4, as shrews are capable of emesis (Ueno et al., 1987) and were believed, through bioinformatics, to have the same B12 binding profile in blood as humans (*vide infra*). Importantly, in the context of modeling the GLP-1 system, the shrew also shows hypoglycemia, anorexia, and emetic sensitivity to existing GLP-1R agonists (Chan et al., 2011; Chan et al., 2013).

RESULTS AND DISCUSSION

Covalent Conjugation of Ex4 to Cbi Retains GLP-1R Agonism *In Vitro*

Here, we present a method, with validation, for corination of Ex4 with the Cbi compound dicyanocobinamide to produce a GLP-1R agonist, namely, Cbi-Ex4 (Figures 1A and 1B), with an half maximal effective concentration (EC_{50}) of ~200 pM in fluorescence resonance energy transfer (FRET) assays that monitor levels of cAMP in HEK-239 cells stably transfected with the human GLP-1R (Figure 1C). The conjugate is linked between the K12 residue of Ex4 and the terminal f-branch of Cbi. These two positions were previously reported by us (Mietlicki-Baase et al., 2018) and others (Równicki et al., 2017; Wierzba et al., 2019) to support high-efficiency conjugation. While no spacer optimization was conducted, we utilized a spacer length that was already established by us to yield a high-potency B12-Ex4 conjugate (Clardy-James et al., 2013).

Cbi-Ex4 Binds to Shrew HC and Displays Improved Half-Life *In Vivo*

Initially, we confirmed the presence of both HC and TC in shrew blood by performing radio-^{57}Co-B12 binding assays and serum B12 protein isolation and identification (see Table S1). In addition to confirming the presence of HC (and separately TC, the profile found in humans, but not rodents [Hygum et al., 2011]), we showed that the total blood B12 binding in *S. murinus* was ~12 nM, of which ~4.5 nM was due to apo-HC. We also demonstrate that, as hypothesized, only HC (K_a 0.45 nM Cbi-Ex4 versus 0.036 nM for Cbi), not TC (K_a for Cbi-Ex4 > 0.2 μM), binds Cbi-Ex4, and that such binding to HC was ~10-fold lower in affinity than for Cbi alone (see Figure S1).

Cbi-Ex4 exhibited reduced plasma clearance (as evidenced by the area under the curve [AUC] and elimination constants) relative to native Ex4 (Figure 1D; Table S2). This finding is likely due, at least in part, to improved stability of the conjugate to proteolytic activity, as we have demonstrated previously for full-vitamin-B12 conjugates (Bonaccorso et al., 2015), and/or reduced renal clearance, both major routes of Ex4 clearance *in vivo* (Copley et al., 2006; Simonsen et al., 2006). ELISA-based pharmacokinetic studies demonstrated that Cbi-Ex4 had a reduced rate of elimination as evidenced by the elimination constants (K_e) of 0.034 h^{-1} for Cbi-Ex4 versus 0.047 h^{-1} for Ex4, and reduced clearance (0.0044 L/h for Cbi-Ex4 versus 0.0056 L/h for Ex4) with no significant difference in volume of distribution between either drug (see Table S2). Overall, Cbi-Ex4 provided greater drug exposure over time, as evidenced by the greater $AUC_{0\text{-}360}$ (2.82 mg*h/L for Ex4 versus 4.55 mg*h/L for Cbi-Ex4), all above the values reported for the 50 nmol/kg dose (Figure 1D; Table S2). We noted also that the C_{max} values for both the 25 nmol/Kg and 50 nmol/Kg doses of Cbi-Ex4 were 17.25 and 30.96 nmol/L (4- to 7-fold greater than the maximum apo-HC levels measured and recorded above), suggesting that the effects of corination are due to the Cbi itself, and are not primarily dependent on binding to HC (the only known binder of Cbi) *in vivo*. At this point it is interesting to note that Herbert and Herzlich (1983) first suggested that HC may play a role in *removing* corrinoids from the human brain, an idea supported by subsequent work by Hansen et al. (1985), who showed HC was found in human colony stimulating factor (CSF; CSF-HC) at concentrations ranging from 10 to 41 pmol/L (median 21 pmol/L; Hansen et al., 1985) with plasma/CSF ratios suggesting such HC was produced in the CNS directly. Overall, the results described herein then may be a consequence of naturally less penetrance of Cbi-Ex4 due to the presence of the highly polar Cbi group, a lack of facilitated transport into the brain for Cbi-Ex4, and/or binding by CSF-HC and subsequent removal or deactivation of Cbi-Ex4 in the CNS. In regard to the latter point, we subsequently assayed HC-Cbi-Ex4 at the GLP-1R and noted an EC_{50} of ~3 nM, essentially rendering a physiologically irrelevant construct (see Figure S2).

Cbi-Ex4 Enhances Glucose Clearance but Does Not Affect Feeding Behavior

Glucose-stimulated insulin secretion following administration of a GLP-1 analog is mediated principally by activation of GLP-1Rs expressed on pancreatic β-cells (Chambers et al., 2017; Lamont et al., 2012; Smith et al., 2014). Therefore, as a proof of concept, we first tested whether Cbi-Ex4 retains its *in vivo* ability to reduce blood glucose following an intraperitoneal (i.p.) glucose tolerance test (IPGTT) across different doses compared to equimolar doses of native Ex4. We observed that shrews treated with Cbi-Ex4 and native Ex4 display improved glucose clearance following i.p. glucose administration compared to vehicle injections (Figures 2A–2C). Furthermore, the plasma glucose clearing rate of Cbi-Ex4 did not differ from the relative equimolar dose of native Ex4 following acute administration, which is indicative of a retained glucoregulatory potency (Figures 2B–2D and S3).

Based on these observations, we then further hypothesized that Cbi-Ex4 may also retain a plasma glucose-lowering action for a longer duration compared to native Ex4. Therefore, a "delayed" IPGTT was performed, in which an i.p. glucose bolus was administered 360 min *after* drug administration to determine whether a longer time window exists for Cbi-Ex4 to facilitate glucose clearance relative to native Ex4. Results show a significant suppression in plasma glucose concentrations 6 h following

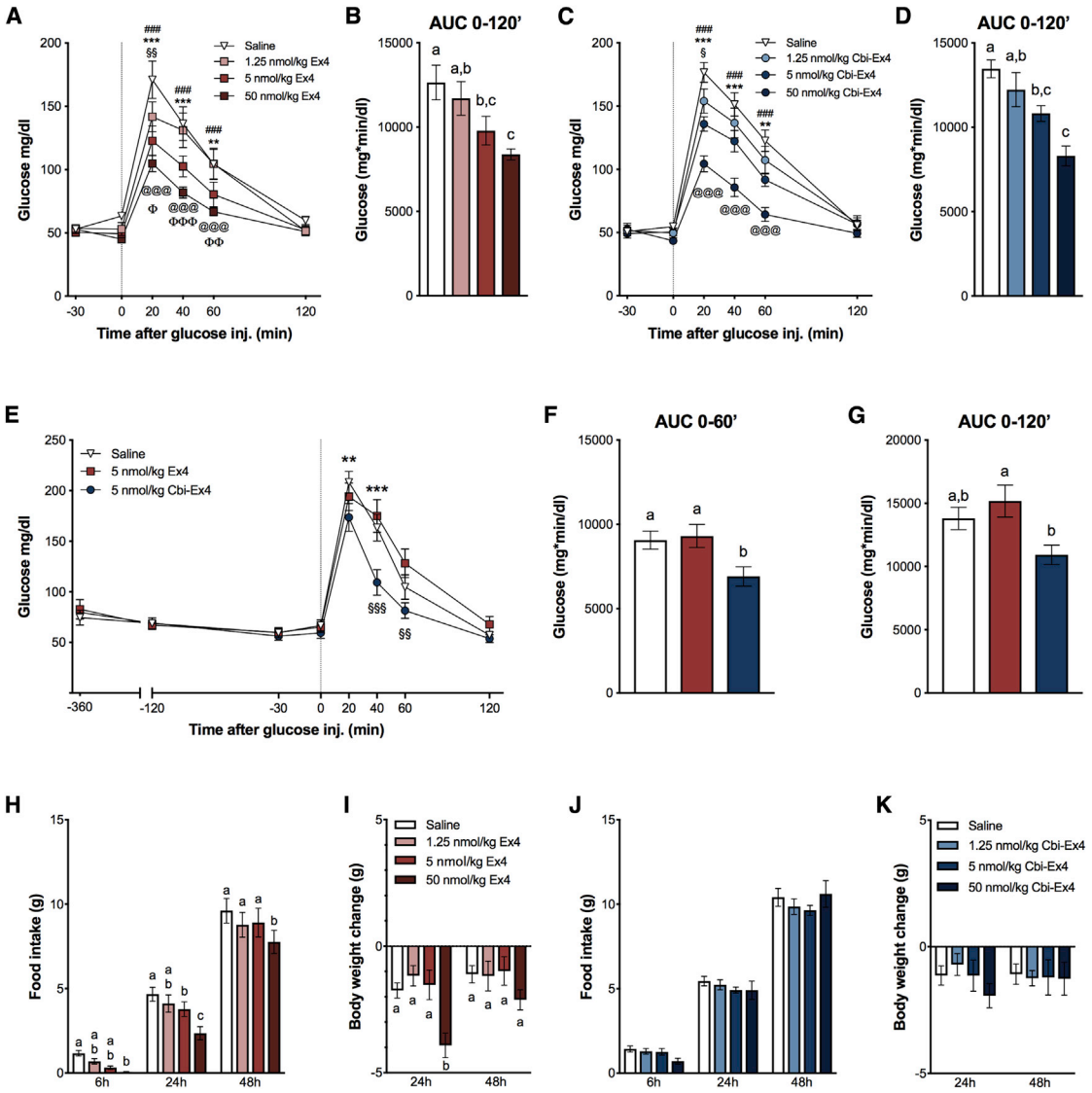

Figure 2. Cbi-Ex4 Enhances Glucose Clearance but Does Not Affect Feeding Behavior

(A) Ex4 (1.25, 5, and 50 nmol/kg, i.p.; i.e., ~5, 20, and 200 μg/kg; respectively) dose-dependently suppressed blood glucose (BG) levels following glucose administration (2 g/kg, i.p.). Saline versus 5 nmol/kg Ex4: **p < 0.01, ***p < 0.001; saline versus 50 nmol/kg Ex4: ###p < 0.001; saline versus 1.25 nmol/kg Ex4: §§p < 0.01; 1.25 nmol/kg Ex4 versus 50 nmol/kg Ex4: @@@p < 0.001; 1.25 nmol/kg Ex4 versus 5 nmol/kg Ex4: Φp < 0.05, ΦΦp < 0.01, ΦΦΦp < 0.001.

(B) Area under the curve (AUC) from 0 (i.e., post-glucose bolus) to 120 min after Ex4.

(C) In an IPGTT Cbi-Ex4 dose-dependently reduced BG levels comparably to equimolar doses of Ex4. Saline versus 5-nmol/kg Cbi-Ex4: **p < 0.01, ***p < 0.001; saline versus 50 nmol/kg Cbi-Ex4: ###p < 0.001; saline versus 1.25 nmol/kg Cbi-Ex4: §p < 0.05; 1.25 nmol/kg Cbi-Ex4 versus 50 nmol/kg Cbi-Ex4: @@@ p < 0.001.

(D) AUC from 0 to 120 min following Cbi-Ex4.

(E) In a delayed glucose load IPGTT, Ex4, Cbi-Ex4 (5 nmol/kg) or vehicle were injected 6 h before glucose load. While Ex4-treatment was no longer effective in reducing BG levels, Cbi-Ex4 retained its BG lowering properties; saline versus Cbi-Ex4: **p < 0.01, ***p < 0.001; Ex4 versus Cbi-Ex4: §§p < 0.01), §§§p < 0.001.

(F and G) AUC analyses from 0 to 60 min and 0 to 120 min, respectively. Cbi-Ex4-treated animals had lower AUC 0-120 compared to Ex4-treated animals and a lower AUC 0–60 compared to Ex4-treated animals and controls.

(H and I) Ex4 dose-dependently induced anorexia leading to weight loss.

(J and K) Equimolar doses of Cbi-Ex4 had no effect on food intake or body weight. All data expressed as mean ± SEM.

Data in (A), (B), (E), and (H)–(K) were analyzed with repeated-measurements two-way ANOVA followed by Tukey's *post hoc* test. Data in (B), (D), (F), and (G) were analyzed with repeated-measurements one-way ANOVA followed by Tukey's *post hoc* test. Means with different letters are significantly different (p < 0.05).

Cbi-Ex4 administration in an IPGTT, with no effect on plasma glucose tolerance being observed after a 6h time delay of native Ex4 administration (Figures 2E–2G).

Direct activation of GLP-1R expressed in various nuclei of the CNS (including, but not limited to those of the hypothalamus and dorsal vagal complex [DVC]), contributes to the body weight and

food intake suppressive effects of exogenously administered first-generation GLP-1R agonists (Kanoski et al., 2011; Mietlicki-Baase et al., 2018; Secher et al., 2014; Sisley et al., 2014). Indeed, both liraglutide and Ex4 penetrate into the CNS and activate GLP-1R-expressing nuclei to induce hypophagia and body weight loss (Chambers et al., 2017; Kanoski et al., 2011; Mietlicki-Baase et al., 2018). In line with previous reports (Chan et al., 2013), systemic administration of native Ex4 produced a strong hypophagic response in the shrew, leading to body-weight loss in a dose-dependent fashion (Figures 2H–2I). This effect is due in part to the ability of native Ex4 to significantly increase the latency of the shrew to initiate feeding compared to vehicle injections (Figure S3). In contrast, Cbi-Ex4 did not significantly affect 24 h food intake or latency to eat, suggesting a lack of neural activation within the CNS (Figures 2J–2K).

Reduced caloric intake and body weight may be viewed as positive therapeutic outcomes in many T2DM patients prescribed existing GLP-1-based therapeutics (i.e., in those patients with accompanying obesity); however, there is a substantial number of T2DM patients that require glycemic control without weight loss. Indeed, in the Western world, 5%–15% of the patients diagnosed with T2DM have a body mass index (BMI) of 25 or lower (Centers for Disease Control and Prevention, 2004; George et al., 2015; Hartmann et al., 2017). The prevalence of T2DM in lean subjects seems to be even higher in some Asiatic countries and among American ethnic minorities (Coleman et al., 2014; Mohan et al., 1997). In addition, there are also diabetic patients suffering from life-threatening diseases or medical treatments including, but not limited to cystic fibrosis (Moheet and Moran, 2017), cancer (Gallo et al., 2018), HIV (Noubissi et al., 2018), chronic heart failure (Nasir and Aguilar, 2012), or COPD (Gläser et al., 2015). Indeed, the prevalence of T2DM in COPD patients is ~20% with an incidence for COPD of ~10% in the overall diabetic population (Caughey et al., 2010; Kerr et al., 2007; Mannino et al., 2008). Further, depending on the tumor type, between 8% and 18% of the cancer patients at the time of diagnosis also suffer from T2DM (Gallo et al., 2018; van de Poll-Franse et al., 2007), and 30%–40% of hospitalized heart-failure patients are diabetic (Echouffo-Tcheugui et al., 2016). This subgroup of T2DM patients is already at increased risk for cachexia, nausea/malaise, and unintended weight loss (von Haehling et al., 2016; von Haehling and Anker, 2014). In these T2DM patients, as well as overweight/obese T2DM patients that cannot effectively tolerate the nausea/emesis of existing GLP-1-based therapeutics, the data provided here support the hypothesis that the Cbi-Ex4 construct can improve glycemic control without producing anorexia and drug-treatment-induced malaise.

Emetic Episodes Are Significantly Reduced Following Cbi-Ex4 Treatment Compared to Native Ex4, Indicative of Improved Tolerance

The most common side effects of all existing FDA-approved GLP-1R agonists are nausea, vomiting, and malaise, with approximately 20%–50% of T2DM patients that had been prescribed GLP-1-based medication, experiencing nausea and/or vomiting (Bergenstal et al., 2010; Buse et al., 2004; DeFronzo et al., 2005; John et al., 2007; Kendall et al., 2005). These adverse events are surprisingly under-investigated, as they limit the widespread use, efficacy, and potential ubiquitous utility of existing GLP-1R agonists for treating metabolic disease. Notably, GLP-1-mediated malaise is not caused by GLP-1-mediated vagal afferent signaling, but is rather promoted by direct central GLP-1R activation (Kanoski et al., 2012), primarily in the brainstem. We therefore hypothesized that the conjugation of Cbi to Ex4 would modify CNS penetrance of Ex4, due to the B12-selective transport system involving TC binding (and the receptor CD320), a system that does not specifically support Cbi binding/transport in general (Mietlicki-Baase et al., 2018), and specifically not in the case of Cbi-Ex4 as measured herein (see Table S1 and Figure S1).

Ex4 dose-dependently induced emesis with the majority of the shrews experiencing emesis after 5- and 50-nmol/kg Ex4 dosing (Figure 3A). Indeed, 29% of the animals exhibited emesis upon administration of the lowest dose of native Ex4, 79% with the intermediate one, and 93% with the highest dose tested. All doses of native Ex4 triggered emesis within minutes after administration (1.25 nmol/kg Ex4: 21 ± 15; 5 nmol/kg Ex4: 10 ± 5 min; 50 nmol/kg: 12 ± 5 min, Figure 3B). In contrast to the profound emesis observed after Ex4, both the prevalence and the number of emetic episodes following equimolar injections of Cbi-Ex4 were significantly reduced (5 nmol/kg Ex4 versus Cbi-Ex4: $p = 0.005$, 50 nmol/kg Ex4 versus Cbi-Ex4: $p = 0.0003$; Figure 3C). Only one shrew experienced emesis after 1.25 nmol/kg Cbi-Ex4 (i.e., 7%), 28% after 5 nmol/kg Cbi-Ex4, and 64% after 50 nmol/kg Cbi-Ex4. In animals that displayed emesis after Cbi-Ex4 treatment, the latency was similar to native Ex4 (Figure 3D). However, the severity and occurrence of the emetic episodes was less severe, as represented by the heatmaps of Ex4 and Cbi-Ex4 depicting emetic intensity and latency for each individual animal across time (Figures 3E, 3F, and S4). These differences are particularly striking at the 5 nmol/kg dose of Cbi-Ex4, which shows a virtual absence of emetic events with the concurrence of strong glycemic effects (see also Figures S3 and S4). Thus, the conjugation of Ex4 to Cbi renders a GLP-1R agonist that, at pharmacological doses, retains glucoregulatory ability without CNS-mediated emesis.

Further support for this hypothesis is found by the near absence of c-Fos protein immunofluorescence (i.e., neuronal activation) in the DVC by Cbi-Ex4 compared to the robust c-Fos activation by native Ex4 (Figure 3G). The DVC is a set of brainstem nuclei (comprised of the nucleus tractus solitarius [NTS], area postrema [AP], and dorsal motor nucleus of the vagus) implicated in regulation of food intake and the processing of aversive stimuli and emetic events (Grill and Hayes, 2012; Hesketh, 2008; Horn, 2014; Miller and Leslie, 1994). Figures 3G and 3H show that systemic native Ex4 induces robust c-Fos expression in both the NTS and AP, whereas an equimolar dose of Cbi-Ex4 did not significantly induce greater c-Fos expression compared to vehicle injections.

Despite Not Affecting Feeding Behavior, Albiglutide Triggers Profound Emesis

Finally, as an additional reference control, we performed a set of studies investigating the emetogenic, anorectic, and

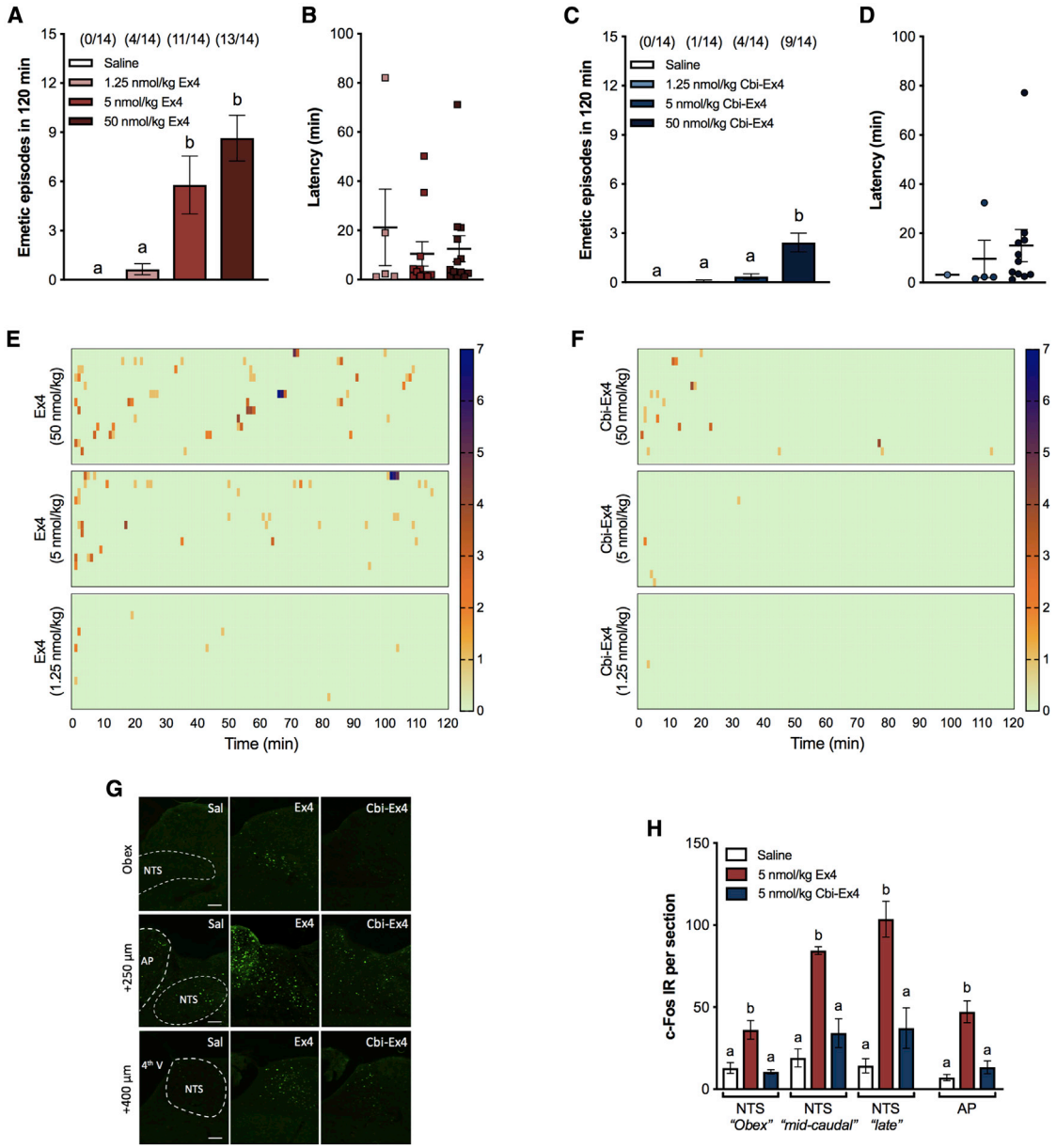

Figure 3. Emetic Episodes Are Significantly Reduced Following Cbi-Ex4 Treatment Compared to Native Ex4, Indicative of Improved Tolerance

(A) Ex4 (1.25, 5, and 50 nmol/kg) induced emesis during 120 min after injection in a dose-related fashion. The number of animals exhibiting emesis, expressed as a fraction of the total number of animal tested, is indicated above each treatment group.

(B) Latency to the first emetic episode of shrews that exhibited emesis after Ex4 treatment.

(C) Number of shrews experiencing emesis following Cbi-Ex4 (1.25, 5, and 50 nmol/kg) during 120 min after injection. The ratio of animals exhibiting emesis is indicated above each treatment group.

(D) Latency to the first emetic episode of shrews that experienced emesis after Cbi-Ex4 treatment.

(E and F) Heatmaps showing latency, number, and intensity of emesis following Ex4 and Cbi-Ex4 dosing for each individual animal across time.

(G) Representative immunofluorescent images showing c-Fos-positive across different NTS plane levels (0, 250, and 400 µm rostral to the obex) and in the medial part of the AP, 3 h after Ex4 (5 nmol/kg), Cbi-Ex4 (5 nmol/kg), or saline i.p. injection.

(H) Quantification of c-Fos positive neurons in the rostral, medial, and caudal NTS and medial AP. Peripheral Ex4 administration significantly increased the number of c-Fos immunoreactive cells in the AP/NTS of shrews 3 h after injection. The number of c-Fos positive cells in the AP/NTS was significantly lower in Cbi-Ex4-treated animals.

All data expressed as mean ± SEM. Means with different letters are significantly different ($p < 0.05$). Data in (A) and (C) were analyzed with repeated-measurements one-way ANOVA followed by Tukey's *post hoc* test. Data in (H) with one-way ANOVA followed by Tukey's *post hoc* test. Scale bar, 100 µm (G).

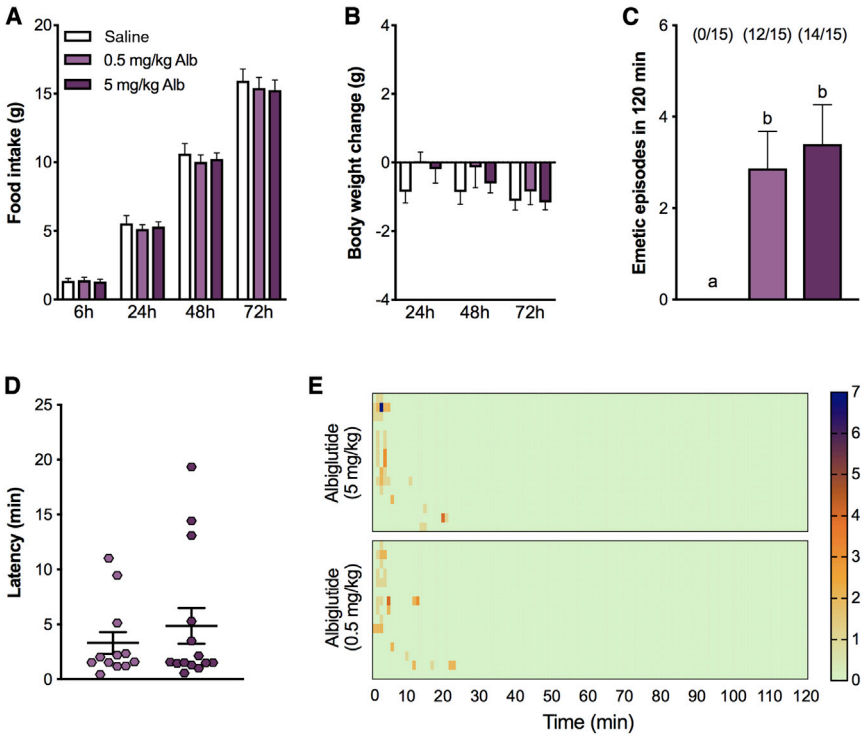

Figure 4. Albiglutide Does Not Cause Anorexia or Body Weight Loss but It Induces Profound Emesis in the Shrew

(A) Number of shrews experiencing emesis and the number of single emetic episodes following albiglutide (0.5 and 5 mg/kg) for 120 min after injection.

(B) Latency to the first emetic episode of shrews that exhibited emesis after albiglutide treatment.

(C) Heatmap showing latency, number, and intensity of emesis for each animal across time.

(D) Food intake at 6, 24, 48, and 72 h post treatment.

(E) Body-weight change at 24, 48, and 72 h after albiglutide or saline treatment. All data expressed as mean ± SEM.

Data in (A) and (B) were analyzed with repeated-measurements one-way ANOVA followed by Tukey's *post hoc* test. Data in (C) and (D) were analyzed with repeated-measurements two-way ANOVA followed by Tukey's *post hoc* test.

body-weight-lowering properties of the long-acting GLP-1 analog albiglutide in our shrew model. This GLP-1-based "macromolecule," consisting of a modified GLP-1 dimer fused to recombinant human albumin, was hypothesized to display minimal brain penetrance due to its size and provide an extended half-life of several days in humans (Rosenstock et al., 2009). Compared to short acting GLP-1 analogs (e.g., Ex4), albiglutide was reported to show reduced incidence of adverse effects (i.e., nausea and vomiting) and with attenuated body-weight-suppressing effects in humans, making it the hoped-for, pre-clinical gold standard for T2DM lean patients (Bettge et al., 2017; Dar et al., 2015; Leiter et al., 2016; Madsbad, 2016; Müller et al., 2019; Prasad-Reddy and Isaacs, 2015; Pratley et al., 2014; Rosenstock et al., 2009).

In line with the reduced anorectic effects of albiglutide previously observed in rodents and humans (Baggio et al., 2004; Pratley et al., 2014), and similarly to Cbi-Ex4, albiglutide at two doses (0.5 and 5 mg/kg) did not cause anorexia and body-weight loss (Figures 4A and 4B) in shrews. Our results demonstrate, however, that both doses of albiglutide induced profound emesis in the majority of shrews tested, albeit with a different temporal profile of emetic responses. The first emetic episode following albiglutide administration occurs within minutes after administration (Figures 4C–4E). This is in direct contrast to comparable doses of Cbi-Ex4 (5 and 0.5 mg/kg of albiglutide correspond to 68 and 6.8 nmol/kg, respectively). While c-Fos following albiglutide treatment was not evaluated in the current study, previous work in rodents demonstrates neuronal activation in nuclei expressing GLP-1Rs, including the AP/NTS following albiglutide systemic delivery (Baggio et al., 2004). Collectively, these data and previous reports suggest that although the whole-brain penetrance may be reduced using a GLP-1R macromolecule agonist like albiglutide, there are still parts of the brain (e.g., AP/NTS) that provide an access point for albiglutide to drive significant adverse effects. Altogether, these results further strengthen the potential future clinical utility that Cbi-Ex4 could have on treating T2DM at doses that do not produce emesis.

Limitations of Study

In summary, by exploiting a biosynthetic precursor of B12 found naturally in humans, but that is inert in the normal physiology of the vitamin, we generated a potent and metabolically stable GLP-1 receptor agonist via corrination, with enhanced and prolonged peripheral glucoregulatory actions at doses that do not affect feeding and, astonishingly, is virtually devoid of emetic responses. Chronic animal studies as well as clinical trials are required to fully elucidate the long-term efficacy and tolerability of Cbi-Ex4. Given the high prevalence of obesity/overweight among T2DM patients, the lack of major effects on feeding and body weight could be considered a negative outcome of the corrination technology. For these patients, "classic" GLP-1R analogs, *if* well tolerated, may be most favorable as weight loss contributes to improved overall health. Nevertheless, our data highlight the incredible potential of corrination, exemplified herein with the development of Cbi-Ex4, as a treatment that would be most beneficial in treating lean T2DM patients, T2DM patients suffering from other comorbidities associated with an anorectic/cachectic state (cancer, COPD, and cystic fibrosis), and T2DM patients seeking glycemic control without emesis.

T2DM and cancer anorexia-cachexia syndrome show similarities in metabolic alterations (Chevalier and Farsijani, 2014; Porporato, 2016). Insulin resistance and reduced glucose tolerance in cancer patients are well-known phenomena. As early as the

1920s, glucose intolerance became a recognized metabolic alteration observed in cancer patients (Petruzzelli and Wagner, 2016). Data from tumor-bearing rodents, partially recapitulating the human clinical state, showed some beneficial effects of Ex4 treatment in attenuating muscle atrophy and in counteracting cancer-induced-insulin-signaling dysregulation (Honors and Kinzig, 2014). However, the CNS-mediated anorectic and emetic effects induced by native Ex4 represents a substantive limitation for possible applications in humans. Cbi-Ex4 could therefore represent an interesting and new GLP-1R-based approach for future investigations into the treatment of cancer-induced insulin resistance.

STAR★METHODS

Detailed methods are provided in the online version of this paper and include the following:

- KEY RESOURCES TABLE
- RESOURCE AVAILABILITY
  - Lead Contact
  - Materials Availability
  - Data and Code Availability
- EXPERIMENTAL MODEL AND SUBJECT DETAILS
  - Cell lines
  - Animals and in vivo study designs
- METHOD DETAILS
  - Drugs
  - Cbi-alkyne synthesis and purification
  - Cbi-Ex4 synthesis and purification
  - Shrew serum total B12, total apo-TC and apo-HC binding capacities
  - HC and TC binding of Cbi-Ex4 and Ex4
  - In vitro GLP-1 binding assay
  - Jugular catheter surgery and pharmacokinetic profile of Ex4 and Cbi-Ex4 in shrews
  - Dose-response effects of Cbi-Ex4 and native Ex4 on glycemic control
  - Direct comparison of pharmacological doses of Cbi-Ex4 and Ex4 on glucoregulation during a standard and a delayed IPGTT
  - Dose-response effects of Ex4 and Cbi-Ex4 on energy balance
  - Direct comparison of pharmacological doses of Cbi-Ex4 and Ex4 on energy balance
  - Emetogenic properties of Ex4 and Cbi-Ex4
  - Direct comparison of pharmacological doses of Cbi-Ex4 and Ex4 on emesis
  - Assessment of neuronal activation in the DVC following Ex4, Cbi-Ex4 or saline treatments
  - Emetogenic properties of albiglutide
  - Effects of albiglutide on energy balance
- QUANTIFICATION AND STATISTICAL ANALYSIS

SUPPLEMENTAL INFORMATION

Supplemental Information can be found online at https://doi.org/10.1016/j.celrep.2020.107768.

ACKNOWLEDGMENTS

The authors gratefully acknowledge Prof. Charles C. Horn (University of Pittsburgh) for his assistance and for the supply of the shrews. This work was supported by the National Institutes of Health (grants NIH–DK–097675 to R.P.D., DK112812 to B.C.D.J., DK097675 to M.R.H., DK115762 to M.R.H., and DK069575 to G.G.H.); the Foundation for Polish Sciences (FNP TEAM POIR.04.04.00–00–4232/17–00 to D.G.); the Swiss National Science Foundation (grants SNF P2ZHP3–178114 and SNF P400PB–186728 to T.B.); and by Xeragenx, St. Louis, Missouri (to R.P.D.).

AUTHOR CONTRIBUTIONS

R.P.D. invented the Cbi-Ex4 technology; T.B., J.L.W., B.C.D.J., M.R.H., and R.P.D. developed the study rationale and experimental designs; T.B., R.P.D., and M.R.H. drafted the manuscript, which was commented on and edited by all authors; T.B. designed and performed most of the *in vivo* experiments with T.B., B.C.D.J., and M.R.H. analyzing the *in vivo* data; J.L.W., I.C.T., and R.P.D. generated the constructs and analyzed the structural data; J.L.W., O.G.C., and I.C.T. performed the *in vitro* experiments with J.L.W., I.C.T., G.G.H., and R.P.D. analyzing the *in vitro* data; E.N. performed the binding studies on TC and HC; S.M.F., L.M.S., A.J.W., D.G., E.N., E.D.S., A.B., and V.A.R.D.S. performed experiments and/or assisted with data analysis; all authors approved the final version of the manuscript.

DECLARATION OF INTERESTS

R.P.D. is a scientific advisory board member and received funds from Balchem Corporation, New Hampton, New York, which were not used in support of these studies. R.P.B. is the named author of a patent pursuant to this work that is owned by Syracuse University. M.R.H. and B.C.D.J. receive funding from Zealand Pharma that was not used in support of these studies. B.C.D.J. receives funding from Pfizer that was not used in support of these studies. M.R.H. receives funding from Novo Nordisk, Eli Lilly & Co. and Boehringer Ingelheim that was not used in support of these studies. All authors declare no other competing financial interests or conflicts of interest.

Received: February 20, 2019
Revised: May 10, 2019
Accepted: May 22, 2020
Published: June 16, 2020

REFERENCES

Ahrén, B., Atkin, S.L., Charpentier, G., Warren, M.L., Wilding, J.P.H., Birch, S., Holst, A.G., and Leiter, L.A. (2018). Semaglutide induces weight loss in subjects with type 2 diabetes regardless of baseline BMI or gastrointestinal adverse events in the SUSTAIN 1 to 5 trials. Diabetes Obes. Metab. *20*, 2210–2219.

Alhadeff, A.L., Holland, R.A., Nelson, A., Grill, H.J., and De Jonghe, B.C. (2015). Glutamate receptors in the central nucleus of the amygdala mediate cisplatin-induced malaise and energy balance dysregulation through direct hindbrain projections. J. Neurosci. *35*, 11094–11104.

Alhadeff, A.L., Mergler, B.D., Zimmer, D.J., Turner, C.A., Reiner, D.J., Schmidt, H.D., Grill, H.J., and Hayes, M.R. (2016). Endogenous glucagon-like peptide-1 receptor signaling in the nucleus tractus solitarius is required for food intake control. Neuropsychopharmacology *42*, 1471–1479.

Baggio, L.L., Huang, Q., Brown, T.J., and Drucker, D.J. (2004). A recombinant human glucagon-like peptide (GLP)-1-albumin protein (albugon) mimics peptidergic activation of GLP-1 receptor-dependent pathways coupled with satiety, gastrointestinal motility, and glucose homeostasis. Diabetes *53*, 2492–2500.

Bergenstal, R.M., Wysham, C., Macconell, L., Malloy, J., Walsh, B., Yan, P., Wilhelm, K., Malone, J., and Porter, L.E.; DURATION-2 Study Group (2010). Efficacy and safety of exenatide once weekly versus sitagliptin or pioglitazone as

an adjunct to metformin for treatment of type 2 diabetes (DURATION-2): a randomised trial. Lancet *376*, 431–439.

Bettge, K., Kahle, M., Abd El Aziz, M.S., Meier, J.J., and Nauck, M.A. (2017). Occurrence of nausea, vomiting and diarrhoea reported as adverse events in clinical trials studying glucagon-like peptide-1 receptor agonists: A systematic analysis of published clinical trials. Diabetes Obes. Metab. *19*, 336–347.

Bonaccorso, R.L., Chepurny, O.G., Becker-Pauly, C., Holz, G.G., and Doyle, R.P. (2015). Enhanced peptide stability against protease digestion induced by intrinsic factor binding of a vitamin B12 conjugate of exendin-4. Mol. Pharm. *12*, 3502–3506.

Buse, J.B., Henry, R.R., Han, J., Kim, D.D., Fineman, M.S., and Baron, A.D.; Exenatide-113 Clinical Study Group (2004). Effects of exenatide (exendin-4) on glycemic control over 30 weeks in sulfonylurea-treated patients with type 2 diabetes. Diabetes Care *27*, 2628–2635.

Caughey, G.E., Roughead, E.E., Vitry, A.I., McDermott, R.A., Shakib, S., and Gilbert, A.L. (2010). Comorbidity in the elderly with diabetes: identification of areas of potential treatment conflicts. Diabetes Res. Clin. Pract. *87*, 385–393.

Centers for Disease Control and Prevention (CDC) (2004). Prevalence of overweight and obesity among adults with diagnosed diabetes—United States, 1988–1994 and 1999–2002. MMWR Morb. Mortal. Wkly. Rep. *53*, 1066–1068.

Chambers, A.P., Sorrell, J.E., Haller, A., Roelofs, K., Hutch, C.R., Kim, K.S., Gutierrez-Aguilar, R., Li, B., Drucker, D.J., D'Alessio, D.A., et al. (2017). The role of pancreatic preproglucagon in glucose homeostasis in mice. Cell Metab *25*, 927–934 e923.

Chan, S.W., Lin, G., Yew, D.T., and Rudd, J.A. (2011). A physiological role of glucagon-like peptide-1 receptors in the central nervous system of Suncus murinus (house musk shrew). Eur. J. Pharmacol. *668*, 340–346.

Chan, S.W., Lin, G., Yew, D.T., Yeung, C.K., and Rudd, J.A. (2013). Separation of emetic and anorexic responses of exendin-4, a GLP-1 receptor agonist in Suncus murinus (house musk shrew). Neuropharmacology *70*, 141–147.

Chepurny, O.G., Bonaccorso, R.L., Leech, C.A., Wöllert, T., Langford, G.M., Schwede, F., Roth, C.L., Doyle, R.P., and Holz, G.G. (2018). Chimeric peptide EP45 as a dual agonist at GLP-1 and NPY2R receptors. Sci. Rep. *8*, 3749.

Chepurny, O.G., Matsoukas, M.T., Liapakis, G., Leech, C.A., Milliken, B.T., Doyle, R.P., and Holz, G.G. (2019). Nonconventional glucagon and GLP-1 receptor agonist and antagonist interplay at the GLP-1 receptor revealed in high-throughput FRET assays for cAMP. J. Biol. Chem. *294*, 3514–3531.

Chevalier, S., and Farsijani, S. (2014). Cancer cachexia and diabetes: similarities in metabolic alterations and possible treatment. Appl. Physiol. Nutr. Metab. *39*, 643–653.

Clardy-James, S., Chepurny, O.G., Leech, C.A., Holz, G.G., and Doyle, R.P. (2013). Synthesis, Characterization and Pharmacodynamics of Vitamin-B12-Conjugated Glucagon-Like Peptide-1. ChemMedChem *4*, 582–586.

Coleman, N.J., Miernik, J., Philipson, L., and Fogelfeld, L. (2014). Lean versus obese diabetes mellitus patients in the United States minority population. J. Diabetes Complications *28*, 500–505.

Copley, K., McCowen, K., Hiles, R., Nielsen, L.L., Young, A., and Parkes, D.G. (2006). Investigation of exenatide elimination and its in vivo and in vitro degradation. Curr. Drug Metab. *7*, 367–374.

Dar, S., Tahrani, A.A., and Piya, M.K. (2015). The role of GLP-1 receptor agonists as weight loss agents in patients with and without type 2 diabetes. Pract. Diabetes *32*, 295–300.

De Jonghe, B.C., and Horn, C.C. (2009). Chemotherapy agent cisplatin induces 48-h Fos expression in the brain of a vomiting species, the house musk shrew (Suncus murinus). Am. J. Physiol. Regul. Integr. Comp. Physiol. *296*, R902–R911.

DeFronzo, R.A., Ratner, R.E., Han, J., Kim, D.D., Fineman, M.S., and Baron, A.D. (2005). Effects of exenatide (exendin-4) on glycemic control and weight over 30 weeks in metformin-treated patients with type 2 diabetes. Diabetes Care *28*, 1092–1100.

Drucker, D.J. (2006). The biology of incretin hormones. Cell Metab. *3*, 153–165.

Drucker, D.J., Sherman, S.I., Bergenstal, R.M., and Buse, J.B. (2011). The safety of incretin-based therapies–review of the scientific evidence. J. Clin. Endocrinol. Metab. *96*, 2027–2031.

Echouffo-Tcheugui, J.B., Xu, H., DeVore, A.D., Schulte, P.J., Butler, J., Yancy, C.W., Bhatt, D.L., Hernandez, A.F., Heidenreich, P.A., and Fonarow, G.C. (2016). Temporal trends and factors associated with diabetes mellitus among patients hospitalized with heart failure: Findings from Get With The Guidelines-Heart Failure registry. Am. Heart J. *182*, 9–20.

Furger, E., Fedosov, S.N., Lildballe, D.L., Waibel, R., Schibli, R., Nexø, E., and Fischer, E. (2012). Comparison of recombinant human haptocorrin expressed in human embryonic kidney cells and native haptocorrin. PLoS ONE *7*, e37421.

Gallo, M., Muscogiuri, G., Felicetti, F., Faggiano, A., Trimarchi, F., Arvat, E., Vigneri, R., and Colao, A. (2018). Adverse glycaemic effects of cancer therapy: indications for a rational approach to cancer patients with diabetes. Metabolism *78*, 141–154.

George, A.M., Jacob, A.G., and Fogelfeld, L. (2015). Lean diabetes mellitus: an emerging entity in the era of obesity. World J. Diabetes *6*, 613–620.

Gimsing, P., and Nexø, E. (1989). Cobalamin-binding capacity of haptocorrin and transcobalamin: age-correlated reference intervals and values from patients. Clin. Chem. *35*, 1447–1451.

Gläser, S., Krüger, S., Merkel, M., Bramlage, P., and Herth, F.J. (2015). Chronic obstructive pulmonary disease and diabetes mellitus: a systematic review of the literature. Respiration *89*, 253–264.

Green, R., Allen, L.H., Bjørke-Monsen, A.L., Brito, A., Guéant, J.L., Miller, J.W., Molloy, A.M., Nexø, E., Stabler, S., Toh, B.H., et al. (2017). Vitamin B_{12} deficiency. Nat. Rev. Dis. Primers *3*, 17040.

Grill, H.J., and Hayes, M.R. (2012). Hindbrain neurons as an essential hub in the neuroanatomically distributed control of energy balance. Cell Metab. *16*, 296–309.

Hansen, M., Brynskov, J., Christensen, P.A., Krintel, J.J., and Gimsing, P. (1985). Cobalamin binding proteins (haptocorrin and transcobalamin) in human cerebrospinal fluid. Scand. J. Haematol. *34*, 209–212.

Hardlei, T.F., and Nexo, E. (2009). A new principle for measurement of cobalamin and corrinoids, used for studies of cobalamin analogs on serum haptocorrin. Clin. Chem. *55*, 1002–1010.

Hartmann, B., Lanzinger, S., Bramlage, P., Groß, F., Danne, T., Wagner, S., Krakow, D., Zimmermann, A., Malcharzik, C., and Holl, R.W. (2017). Lean diabetes in middle-aged adults: a joint analysis of the German DIVE and DPV registries. PLoS ONE *12*, e0183235.

Hayes, M.R., and Schmidt, H.D. (2016). GLP-1 influences food and drug reward. Curr. Opin. Behav. Sci. *9*, 66–70.

Hayes, M.R., De Jonghe, B.C., and Kanoski, S.E. (2010). Role of the glucagon-like-peptide-1 receptor in the control of energy balance. Physiol. Behav. *100*, 503–510.

Hayes, M.R., Leichner, T.M., Zhao, S., Lee, G.S., Chowansky, A., Zimmer, D., De Jonghe, B.C., Kanoski, S.E., Grill, H.J., and Bence, K.K. (2011). Intracellular signals mediating the food intake-suppressive effects of hindbrain glucagon-like peptide-1 receptor activation. Cell Metab. *13*, 320–330.

Hayes, M.R., Mietlicki-Baase, E.G., Kanoski, S.E., and De Jonghe, B.C. (2014). Incretins and amylin: neuroendocrine communication between the gut, pancreas, and brain in control of food intake and blood glucose. Annu. Rev. Nutr. *34*, 237–260.

Herbert, V., and Herzlich, B. (1983). Quantitation of intrinsic factor. Blood *61*, 819.

Hesketh, P.J. (2008). Chemotherapy-induced nausea and vomiting. N. Engl. J. Med. *358*, 2482–2494.

Holst, J.J. (2007). The physiology of glucagon-like peptide 1. Physiol. Rev. *87*, 1409–1439.

Honors, M.A., and Kinzig, K.P. (2014). Chronic exendin-4 treatment prevents the development of cancer cachexia symptoms in male rats bearing the Yoshida sarcoma. Horm. Cancer *5*, 33–41.

Horn, C.C. (2014). Measuring the nausea-to-emesis continuum in non-human animals: refocusing on gastrointestinal vagal signaling. Exp. Brain Res. *232*, 2471–2481.

Horn, C.C., Kimball, B.A., Wang, H., Kaus, J., Dienel, S., Nagy, A., Gathright, G.R., Yates, B.J., and Andrews, P.L. (2013). Why can't rodents vomit? A comparative behavioral, anatomical, and physiological study. PLoS ONE *8*, e60537.

Hygum, K., Lildballe, D.L., Greibe, E.H., Morkbak, A.L., Poulsen, S.S., Sorensen, B.S., Petersen, T.E., and Nexø, E. (2011). Mouse transcobalamin has features resembling both human transcobalamin and haptocorrin. PLoS ONE *6*, e20638.

John, L.E., Kane, M.P., Busch, R.S., and Hamilton, R.A. (2007). Expanded use of exenatide in the management of type 2 diabetes. Diabetes Spectr. *20*, 59–63.

Kanazawa, S., and Herbert, V. (1983). Noncobalamin vitamin B12 analogues in human red cells, liver, and brain. Am. J. Clin. Nutr. *37*, 774–777.

Kanoski, S.E., Fortin, S.M., Arnold, M., Grill, H.J., and Hayes, M.R. (2011). Peripheral and central GLP-1 receptor populations mediate the anorectic effects of peripherally administered GLP-1 receptor agonists, liraglutide and exendin-4. Endocrinology *152*, 3103–3112.

Kanoski, S.E., Rupprecht, L.E., Fortin, S.M., De Jonghe, B.C., and Hayes, M.R. (2012). The role of nausea in food intake and body weight suppression by peripheral GLP-1 receptor agonists, exendin-4 and liraglutide. Neuropharmacology *62*, 1916–1927.

Kanoski, S.E., Hayes, M.R., and Skibicka, K.P. (2016). GLP-1 and weight loss: unraveling the diverse neural circuitry. Am. J. Physiol. Regul. Integr. Comp. Physiol. *310*, R885–R895.

Kendall, D.M., Riddle, M.C., Rosenstock, J., Zhuang, D., Kim, D.D., Fineman, M.S., and Baron, A.D. (2005). Effects of exenatide (exendin-4) on glycemic control over 30 weeks in patients with type 2 diabetes treated with metformin and a sulfonylurea. Diabetes Care *28*, 1083–1091.

Kerr, E.A., Heisler, M., Krein, S.L., Kabeto, M., Langa, K.M., Weir, D., and Piette, J.D. (2007). Beyond comorbidity counts: how do comorbidity type and severity influence diabetes patients' treatment priorities and self-management? J. Gen. Intern. Med. *22*, 1635–1640.

Klarenbeek, J., Goedhart, J., van Batenburg, A., Groenewald, D., and Jalink, K. (2015). Fourth-generation epac-based FRET sensors for cAMP feature exceptional brightness, photostability and dynamic range: characterization of dedicated sensors for FLIM, for ratiometry and with high affinity. PLoS ONE *10*, e0122513.

Kuda-Wedagedara, A.N.W., Workinger, J.L., Nexø, E., Doyle, R.P., and Viola-Villegas, N. (2017). ^{89}Zr-cobalamin PET tracer: synthesis, cellular uptake, and use for tumor imaging. ACS Omega *2*, 6314–6320.

Lamont, B.J., Li, Y., Kwan, E., Brown, T.J., Gaisano, H., and Drucker, D.J. (2012). Pancreatic GLP-1 receptor activation is sufficient for incretin control of glucose metabolism in mice. J. Clin. Invest. *122*, 388–402.

Leiter, L.A., Mallory, J.M., Wilson, T.H., and Reinhardt, R.R. (2016). Gastrointestinal safety across the albiglutide development programme. Diabetes Obes. Metab. *18*, 930–935.

Madsbad, S. (2016). Review of head-to-head comparisons of glucagon-like peptide-1 receptor agonists. Diabetes Obes. Metab. *18*, 317–332.

Mannino, D.M., Thorn, D., Swensen, A., and Holguin, F. (2008). Prevalence and outcomes of diabetes, hypertension and cardiovascular disease in COPD. Eur. Respir. J. *32*, 962–969.

Mietlicki-Baase, E.G., Ortinski, P.I., Rupprecht, L.E., Olivos, D.R., Alhadeff, A.L., Pierce, R.C., and Hayes, M.R. (2013). The food intake-suppressive effects of glucagon-like peptide-1 receptor signaling in the ventral tegmental area are mediated by AMPA/kainate receptors. Am. J. Physiol. Endocrinol. Metab. *305*, E1367–E1374.

Mietlicki-Baase, E.G., Liberini, C.G., Workinger, J.L., Bonaccorso, R.L., Borner, T., Reiner, D.J., Koch-Laskowski, K., McGrath, L.E., Lhamo, R., Stein, L.M., et al. (2018). A vitamin B12 conjugate of exendin-4 improves glucose tolerance without associated nausea or hypophagia in rodents. Diabetes Obes. Metab. *20*, 1223–1234.

Miller, A.D., and Leslie, R.A. (1994). The area postrema and vomiting. Front. Neuroendocrinol. *15*, 301–320.

Mohan, V., Vijayaprabha, R., Rema, M., Premalatha, G., Poongothai, S., Deepa, R., Bhatia, E., Mackay, I.R., and Zimmet, P. (1997). Clinical profile of lean NIDDM in South India. Diabetes Res. Clin. Pract. *38*, 101–108.

Moheet, A., and Moran, A. (2017). CF-related diabetes: containing the metabolic miscreant of cystic fibrosis. Pediatr. Pulmonol. *52* (*S48*), S37–S43.

Müller, T.D., Finan, B., Bloom, S.R., D'Alessio, D., Drucker, D.J., Flatt, P.R., Fritsche, A., Gribble, F., Grill, H.J., Habener, J.F., et al. (2019). Glucagon-like peptide 1 (GLP-1). Mol. Metab. *30*, 72–130.

Nasir, S., and Aguilar, D. (2012). Congestive heart failure and diabetes mellitus: balancing glycemic control with heart failure improvement. Am. J. Cardiol. *110*, 50B–57B.

Noubissi, E.C., Katte, J.C., and Sobngwi, E. (2018). Diabetes and HIV. Curr. Diab. Rep. *18*, 125.

Petruzzelli, M., and Wagner, E.F. (2016). Mechanisms of metabolic dysfunction in cancer-associated cachexia. Genes Dev. *30*, 489–501.

Porporato, P.E. (2016). Understanding cachexia as a cancer metabolism syndrome. Oncogenesis *5*, e200.

Prasad-Reddy, L., and Isaacs, D. (2015). A clinical review of GLP-1 receptor agonists: efficacy and safety in diabetes and beyond. Drugs Context *4*, 212283.

Pratley, R.E., Nauck, M.A., Barnett, A.H., Feinglos, M.N., Ovalle, F., Harman-Boehm, I., Ye, J., Scott, R., Johnson, S., Stewart, M., and Rosenstock, J.; HARMONY 7 study group (2014). Once-weekly albiglutide versus once-daily liraglutide in patients with type 2 diabetes inadequately controlled on oral drugs (HARMONY 7): a randomised, open-label, multicentre, non-inferiority phase 3 study. Lancet Diabetes Endocrinol. *2*, 289–297.

Pratley, R.E., Aroda, V.R., Lingvay, I., Lüdemann, J., Andreassen, C., Navarria, A., and Viljoen, A.; SUSTAIN 7 Investigators (2018). Semaglutide versus dulaglutide once weekly in patients with type 2 diabetes (SUSTAIN 7): a randomised, open-label, phase 3b trial. Lancet Diabetes Endocrinol. *6*, 275–286.

Rosenblatt, D.S., Fenton, W.A., Scriver, C.R., Beaudet, A.L., Valle, D., and Sly, W.S. (2001). Inherited Disorders of Folate and Cobalamin Transport and Metabolism (McGraw-Hill).

Rosenstock, J., Reusch, J., Bush, M., Yang, F., and Stewart, M.; Albiglutide Study Group (2009). Potential of albiglutide, a long-acting GLP-1 receptor agonist, in type 2 diabetes: a randomized controlled trial exploring weekly, biweekly, and monthly dosing. Diabetes Care *32*, 1880–1886.

Równicki, M., Wojciechowska, M., Wierzba, A.J., Czarnecki, J., Bartosik, D., and Gryko, D. (2017). Vitamin B12 as a carrier of peptide nucleic acid (PNA) into bacterial cells. Sci. Rep. *7*, 7644.

Sadry, S.A., and Drucker, D.J. (2013). Emerging combinatorial hormone therapies for the treatment of obesity and T2DM. Nat. Rev. Endocrinol. *9*, 425–433.

Secher, A., Jelsing, J., Baquero, A.F., Hecksher-Sørensen, J., Cowley, M.A., Dalbøge, L.S., Hansen, G., Grove, K.L., Pyke, C., Raun, K., et al. (2014). The arcuate nucleus mediates GLP-1 receptor agonist liraglutide-dependent weight loss. J. Clin. Invest. *124*, 4473–4488.

Sikirica, M.V., Martin, A.A., Wood, R., Leith, A., Piercy, J., and Higgins, V. (2017). Reasons for discontinuation of GLP1 receptor agonists: data from a real-world cross-sectional survey of physicians and their patients with type 2 diabetes. Diabetes Metab. Syndr. Obes. *10*, 403–412.

Simonsen, L., Holst, J.J., and Deacon, C.F. (2006). Exendin-4, but not glucagon-like peptide-1, is cleared exclusively by glomerular filtration in anaesthetised pigs. Diabetologia *49*, 706–712.

Sisley, S., Gutierrez-Aguilar, R., Scott, M., D'Alessio, D.A., Sandoval, D.A., and Seeley, R.J. (2014). Neuronal GLP1R mediates liraglutide's anorectic but not glucose-lowering effect. J. Clin. Invest. *124*, 2456–2463.

Smith, E.P., An, Z., Wagner, C., Lewis, A.G., Cohen, E.B., Li, B., Mahbod, P., Sandoval, D., Perez-Tilve, D., Tamarina, N., et al. (2014). The role of β cell

glucagon-like peptide-1 signaling in glucose regulation and response to diabetes drugs. Cell Metab. *19*, 1050–1057.

Stupperich, E., and Nexø, E. (1991). Effect of the cobalt-N coordination on the cobamide recognition by the human vitamin B12 binding proteins intrinsic factor, transcobalamin and haptocorrin. Eur. J. Biochem. *199*, 299–303.

Ueno, S., Matsuki, N., and Saito, H. (1987). Suncus murinus: a new experimental model in emesis research. Life Sci. *41*, 513–518.

van de Poll-Franse, L.V., Houterman, S., Janssen-Heijnen, M.L., Dercksen, M.W., Coebergh, J.W., and Haak, H.R. (2007). Less aggressive treatment and worse overall survival in cancer patients with diabetes: a large population based analysis. Int. J. Cancer *120*, 1986–1992.

von Haehling, S., and Anker, S.D. (2014). Prevalence, incidence and clinical impact of cachexia: facts and numbers—update 2014. J. Cachexia Sarcopenia Muscle *5*, 261–263.

von Haehling, S., Anker, M.S., and Anker, S.D. (2016). Prevalence and clinical impact of cachexia in chronic illness in Europe, USA, and Japan: facts and numbers update 2016. J. Cachexia Sarcopenia Muscle *7*, 507–509.

Wierzba, A.J., Hassan, S., and Gryko, D. (2019). Synthetic Approaches toward Vitamin B12 Conjugates. Asian Journal of Chemistry *8*, 6–24.

Wysham, C., Blevins, T., Arakaki, R., Colon, G., Garcia, P., Atisso, C., Kuhstoss, D., and Lakshmanan, M. (2014). Efficacy and safety of dulaglutide added onto pioglitazone and metformin versus exenatide in type 2 diabetes in a randomized controlled trial (AWARD-1). Diabetes Care *37*, 2159–2167.

STAR★METHODS

KEY RESOURCES TABLE

REAGENT or RESOURCE	SOURCE	IDENTIFIER
Antibodies		
Alexa fluor 488 Donkey Anti-Rabbit 1gG (H+L)	Jackson Immuno Research	CAT# 711-545-152; RRID:AB_2313584
c-Fos 9F6 Rabbit mAb	Cell Signaling	CAT# s22505; RRID:AB_2247211
Bacterial and Virus Strains		
H188 adenovirus	Lab of Prof. Jees Kalink, Division of Cell Biology, the Netherlands Cancer Institute, Amsterdam, the Netherlands.	N/A
Biological Samples		
Shrew brain	In house (University of Pennsylvania)	N/A
Shrew blood	In house (University of Pennsylvania)	N/A
Chemicals, Peptides, and Recombinant Proteins		
Exendin-4	Bachem	CAT # H-8730
Cbi-Exendin-4	This paper	N/A
Albiglutide	AdooQ Bioscience	CAT# A16823
aCSF	Harvard Apparatus	CAT# 59-7316
Vitamin B_{12}	Sigma-Aldrich	CAT# V2876
Dicyanocobinamide	Sigma-Aldrich	CAT#C3021
1,1′-Carbonyl-di-(1,2,4-triazole)	Sigma-Aldrich	CAT# 21861
1-Amino-3-butyne	Sigma-Aldrich	CAT# 715190
Fetal Bovine Serum	Sigma-Aldrich	CAT# 12303C
Dulbecco's Modified Eagle Medium	Sigma-Aldrich	CAT# D6429
Penicillin-Streptomycin	ThermoFisher Scientific	CAT# 15140122
G-418 Disulfate Salt Solution	Sigma-Aldrich	CAT# G8168
Bovine Serum Albumin	Sigma-Aldrich	CAT# A7030
Sodium Chloride	Fisher Scientific	CAT# BP358-1
Potassium Chloride	Fisher Scientific	CAT# BP366
Magnesium Chloride Hexahydrate	Fisher Scientific	CAT# BP214
Calcium Chloride Dihydrate	Fisher Scientific	CAT# BP510
HEPES	Sigma-Aldrich	CAT# H0887
Trypsin-EDTA	ThermoFisher Scientific	CAT# 25200072
Activated Charcoal	Sigma-Aldrich	CAT#C5197
Bovine hemoglobin	Sigma Aldrich	CAT#H2500
^{57}Co-B12	KemEnTec	N/A
0.1% Human albumin	Sigma Aldrich	CAT#A9731
^{22}Na	GE Healthcare Europe	N/A
Critical Commercial Assays		
Ex4 ELISA kit	Phoenix Pharmaceuticals	EK-070-94
Experimental Models: Cell Lines		
HEK293 Stably Transfected with hGLP1-R	Generated in-house, SUNY, Upstate Medical University	N/A
Experimental Models: Organisms/Strains		
Adult male shrews (*Suncus murinus*)	UPMC Hillman Cancer Center	N/A
Software and Algorithms		
GraphPad PRISM	GraphPad Software	RRID: SCR_000306
Illustrator (CS6)	Abobe	RRID: SCR_010279

(*Continued on next page*)

Continued

REAGENT or RESOURCE	SOURCE	IDENTIFIER
Other		
Feline diet	PMI Lab Diets	CAT# 5003
Ferret diet	PMI Lab Diets	CAT# 5L14
Silicone tubing	SAI Infusion Technologies	CAT# Sku SIL-3-25
Glucose test strips OneTouch Ultra Blue	CVS	NA

RESOURCE AVAILABILITY

Lead Contact

Further information and requests for resources and reagents should be directed to and will be fulfilled by the Lead Contact, Robert P. Doyle (rpdoyle@syr.edu).

Materials Availability

This study generated new unique reagents. RP Doyle is the named author of a patent pursuant to this work that is owned by Syracuse University and will supply the reagent under MTA upon request.

Data and Code Availability

The published article includes all data generated or analyzed during this study. No code was used or generated in this study

EXPERIMENTAL MODEL AND SUBJECT DETAILS

Cell lines

HEK293 cells stably expressing the human GLP-1R at a density of 150,000 receptors/cell were obtained from Novo Nordisk A/S (Bagsvaerd, Denmark) by GGH. HEK293 cells stably expressing H188 were generated by O.G. Chepurny in the Holz laboratory (Chepurny et al., 2018). All cell cultures were maintained in Dulbecco's Modified Eagles Medium (DMEM) containing 25 mM glucose and supplemented with 10% fetal bovine serum (FBS) and 1% penicillin-streptomycin. Cell cultures equilibrated at 37 C in a humidified incubator with 5% CO_2 were passaged twice a week.

Animals and in vivo study designs

Adult male shrews (*Suncus murinus*) weighing ~50-80 g (n = 156 total), where obtained from Dr. Charles Horn, University of Pittsburgh. These animals were offspring from a colony maintained at the University of Pittsburgh Cancer Institute (a Taiwanese strain derived from stock supplied by the Chinese University of Hong Kong).

Animals were single housed in plastic cages (37.3 × 23.4 × 14 cm, Innovive) under a 12-hour:12-hour light/dark cycle in a temperature- and humidity- controlled environment. Animal were fed *ad libitum* with a mixture of feline (75%, Laboratory Feline Diet 5003, Lab Diet) and mink food (25%, High Density Ferret Diet 5LI4, Lab Diet) and had *ad libitum* access to tap water except where noted.

Shrews were habituated to single housing in their home cage and IP injections at least 1 wk prior to experimentation. All animals were naive to any experimental drug and test prior to the beginning of the experiment. All experimental injections were separated by at least 72h. For most *in vivo* experiments, injections were administered using a within-subjects, Latin square design. The exceptions were the pharmacokinetic and the immunohistochemical studies, which were conducted in a between-subjects design. All procedures were approved by the Institutional Care and Use Committee of the University of Pennsylvania.

METHOD DETAILS

Drugs

CN_2Cbi was purchased from Sigma-Aldrich. K12-azido modified Ex4 was produced by NeoScientific (Cambridge, USA). Cbi-conjugated exendin-4 (Cbi-Ex4) was synthesized, characterized and screened as described below. For all *in vivo* studies Cbi-Ex4, Ex4 (Bachem), and albiglutide (AdooQ Bioscience, Cat. No. A16823) were dissolved in 0.9% saline. In all studies, except in the pharmacokinetic study, Ex4 (1.25, 5 and 50 nmol/kg; i.e., ~5, 20 and 200 μg/kg; respectively), Cbi-Ex4 (equimolar dose to Ex4), and albiglutide (0.5 and 5 mg/kg) were administered intraperitoneally (IP). For the pharmacokinetic study, Ex4 (25 and 50 nmol/kg) and Cbi-Ex4 (equimolar doses to Ex4) were infused intravenously (IV) (see details below).

Cbi-alkyne synthesis and purification

$(CN)_2$Cbi (0.077 mmol; 80 mg; 1 equiv.) and CDT (1,1′-carbonyl-di-(1,2,4-triazole); 1.535 mmol; 252 mg, 20 equiv.) were dissolved in dry N-Methyl-2-pyrrolidone (NMP, 2.5 mL) at 40°C under an argon atmosphere. The resulting solution was stirred for 30 min at 40°C (full conversion of Cbi to Cbi-CDT adduct was achieved over this time (as established by RP-HPLC). Subsequently, the aminoalkyne (NH_2-C2-alkyne, 126 μL, 20 equiv.) and triethylamine (TEA, 20 μL) were added under an argon atmosphere. The resulting solution was stirred at 40°C for 1h. After this time the conversion (monitored by RP-HPLC) was not complete, thus another portion of the amino-alkyne (126 μL, 20 equiv.) and TEA (20 μL) were added and the mixture was stirred for an additional hour at 40°C. The reaction mixture was subsequently poured into ethyl acetate (50 mL), and centrifuged (the residue being transferred with a minimal amount of MeOH into ethyl acetate). After complete precipitation, the solid was dissolved in 2 mL of MeOH and precipitated with diethyl ether (50 mL). The crude solid was dissolved in water and purified via preparative HPLC (see supplementary details for full synthetic details and characterization).

Cbi-Ex4 synthesis and purification

To a 5mL round bottom flask containing a stir bar, copper (I) iodide (Cu(I)I) (3.3 mg, 0.017 mmol), and tris[(1-benzyl-1H-1,2,3-triazol-4-yl)methyl]amine (TBTA) (7.0 mg, 0.013 mmol) was added to 500 μL of 4:1 DMF:H_2O. The reaction mixture was allowed to stir at room temperature until a color change occurred (clear to yellowish brown) (∼15 min). The solution was treated with K12-azido-exendin-4 (2.0 mg, 0.0004 mmol) and Cbi-alkyne (4.8 mg, 0.004 mmol) and allowed to stir overnight (Figure 1A). The product was purified using Shimadzu Prominence HPLC using a C18 column (Eclipse XDB-C18 5 μm, 4.6 × 150 mm) with H_2O + 0.1% TFA and acetonitrle. t_R (RP-HPLC, from 1% CH_3CN/H_2O + 0.1% to TFA to 70% % CH_3CN/H_2O + 0.1% to TFA in 15 min): 11.2 min. ESI-MS shows the expected *m/z* 5354, observed *m/z* = 1339 $[M+4H]^{+4}$, 1071 $[M+5H]^{+5}$(Figure 1B).

Shrew serum total B12, total apo-TC and apo-HC binding capacities

Pool of shrew serum from two animals (1 and 2) as: 3 × 150 μl animal 1 + 2 mixed, 3 × 150 μl animal 1 only, 3 × 150 μl animal 2 only were assayed as previously described (Gimsing and Nexø, 1989). Briefly, total B12 was measured using serum diluted 1:5 with 0.9% NaCl on the automatic platform Advia Centaur CP Immunoassay system. Unsaturated B12 binding capacity was measured on serum diluted 1:10 employing coated charcoal to separate free and bound ^{57}Co-B12 (KemEnTec) to separate TC and HC. A sample saturated with ^{57}Co-B12 was run on a Superdex® 200 HR 10/30 column (GE Healthcare Europe) using a Dionex® ICS-3000 chromatograph (Dionex Corporation), eluted at a flow rate of 400 μL/min for approx. 70 min employing a Tris buffer (0.1 mol/L) (Sigma Aldrich), 1 mol/L NaCl (Merck), 0.5 g/L bovine albumin (Sigma Aldrich), 0.2 g/L sodium-azide (Merck), pH 8.0. The eluted fractions were counted in a Wizard Automatic Gamma Counter to monitor the elution of ^{57}Co-B12. Molecular mass markers Blue Dextran (Sigma Aldrich) and ^{22}Na (GE Healthcare Europe) were used for determination of void volume (V_o), and total volume (V_t).

HC and TC binding of Cbi-Ex4 and Ex4

HC and TC binding assays were conducted as previously reported (Stupperich and Nexø, 1991). In brief, typically 50 pmol ^{57}Co-B12 (KemEnTec) was mixed with Cbi-Ex4 and the binding protein (HC or TC) was added in a concentration between 25-40 pmol/l. The total incubation volume was 0.375 ml, with 0.1 M sodium phosphate and 0.1% human albumin (Sigma-Aldrich), pH 8. The mixture was equilibrated at 4°C for 20 h. Free versus protein bound corrinoids (cyanocobalamin versus Cbi-Ex4) were separated by precipitating with hemoglobin-coated charcoal previously prepared by mixing equal volumes of a 5% aqueous suspension of activated charcoal (Sigma-Aldrich) with a 0.5% aqueous solution of bovine hemoglobin (Sigma-Aldrichk). Protein-bound [^{57}Co-B12] was then measured in a multichannel counter (Merlsgaard, DK).

In vitro GLP-1 binding assay

Agonism at the GLP-1R of Ex4 and Cbi-Ex4, was monitored using HEK293 cells stably transfected with the human GLP-1 receptor. The cells were cultured in Dulbecco's Modified Eagle Medium (DMEM) with 10% FBS, 1% pen/strep and 250 μg/mL geneticin/g-418. HEK293 cells stably transfected with GLP-1R were seeded at ∼8.5x10^5 cells/mL in 12 mL in DMEM in a 100 mm x 20 mm sterile tissue culture dish (TCD). Within 24h of seeding the TCD is ∼80% confluent and infected with the H188 adenovirus, the most sensitive cAMP FRET reporter (Klarenbeek et al., 2015), and incubated for 20h prior to screening. Cells, now infected with the H188 adenovirus, were grown to > 95% confluency at which time they were removed from cultured media and placed in 96-well clear-bottom assay plate (Costar 3904, Corning, NY) in 200 μL/well of a standard extracellular saline (SES) solution supplemented with 11 mM glucose and 0.1% BSA. Real-time kinetic FRET assays were performed using a FlexStation 3 Multi-Mode Microplate Reader. Assays were performed at 25°C, over 400 s with subsequent stimulant injections of Ex4 and Cbi-Ex4 concentrations ranging from 3 pM to 1 nM (see Figure 1C, inset) at 100 s, with emission measurements every 6 s. To determine agonism, an increase in 485/535 nm FRET ratio was monitored indicating increase of cAMP concentration through cAMP binding to an exchange protein directly activate by cAMP (EPAC) (Klarenbeek et al., 2015).

Jugular catheter surgery and pharmacokinetic profile of Ex4 and Cbi-Ex4 in shrews

Shrews (n = 15) were deeply anesthetized with a cocktail of ketamine, (180 mg/kg; Butler Schein), xylazine (5.4 mg/kg; Anased), and acepromazine (1.28 mg/kg; Butler Schein). Homemade silicone catheters (9 cm-long, 3Fr, ID 0.56 mm, OD 1 mm, cat. Sku SIL-3-25,

SAI Infusion Technologies) were pre-filled with bacteriostatic saline 5 IU/mL heparin solution (Butler Schein). A 3 cm-long incision in the interscapular region and a 2 cm-long incision from the right mandible toward the shoulder were made without cutting any underlying tissue. A subcutaneous route was cleared between the incision sites and the catheter was threaded over the shoudler of the animal through the cleared path and fixed to a round mesh back-mount that was implanted subcutaneously between the shoulder blades. The tissue underlying the ventral neck incision was gently dissected using forceps to expose the right jugular vein. The exposed jugular vein was stretched and tied off toward the surface of the incision and using a flat spatula. Using microsurgical scissors a partial perpendicular incision was made and microsurgical forceps were used to insert the catheter through the incision and gently inserted 1 cm (a small silicone ball of sealant glue attached to catheter used as stop guide) into the vein. Cannua placement and patency were verified by drawing up vein blood with a syringe attached to the catheter before the cathether was sealed with metal obturator. The catheter was secured to the vein by tying two sutures (4-0, silk) around the catheter above and below the silicone ball. Sutures were tied together and acyrlic glue was placed over the insertion point to secure the catheter in place. Incisions were closed with simple interrupted sutures (4-0, silk) and all animals received 2 mL of warm saline and analgesic (Meloxicam, 5mg/kg, IP, Boehringer Ingelheim). To prevent infection and maintain patency, catheters were flushed daily with 0.05 mL of the antibiotic Timentin (0.93 mg/mL; Fisher) dissolved in heparinized saline solution (5 IU/mL), except for the testing days in which the catheters were flushed with heparinized saline only 30 min prior drug administration.

Three hours before dark onset, shrews were briefly anesthetized with isoflurane (Henry Schein Animal Health) and 50 μL of blood were collected from their tail into a heparin container (t = −10). Immediately after, each shrew received a bolus IV infusion of either Ex4 (100 and 200 μg/kg [i.e., 25, 50 nmol/kg; respectively]), or equimolar doses Cbi-Ex4. Subsequent blood collection occurred at 5, 45, 90, 135, 180, 270 and 360 min post IV infusion. Plasma was obtained by spinning blood at 6000 g for 6 min and subsequently stored at −80°C. Concentrations of Ex4 and Cbi-Ex4 were measured using a commercial kit purchased from Phoenix Pharmaceuticals (Exendin-4 (*Heloderma suspectum*) EK-070-94). The ELISA was performed according to the manufacturer's protocol with the exception of shrew blood serum that had been dosed with Cbi-Ex4. A Cbi-Ex4 standard curve was generated by matching concentrations provided by the manufacturer's standards.

Dose-response effects of Cbi-Ex4 and native Ex4 on glycemic control

The protocol for performing an intraperitoneal glucose tolerance test (IPGTT) in shrews was similar to that previously used in rodents (Mietlicki-Baase et al., 2018). Two hours before dark onset, shrews were food- and water- deprived. Three hours later, baseline blood glucose levels were determined from a small drop of tail blood and measured using a standard glucometer (AccuCheck). Immediately following, each shrew (n = 10) received IP injection of Ex4 (1.25, 5 or 50 nmol/kg) or vehicle (1 mL/100 g BW sterile saline). BG was measured 30 minutes later (t = 0 min), then each shrew received an IP bolus of glucose (2 g/kg). Subsequent BG readings were taken at 20, 40, 60 and 120 min after glucose injection. After the final BG reading, food and water were returned. IPGTT studies were carried out in a within-subject, counter-balanced design and separated by 7 days. In another cohort of animals (n = 11), the same paradigm was applied but each shrew received IP injection of Cbi-Ex4 (1.25, 5 or 50 nmol/kg) or vehicle instead.

Direct comparison of pharmacological doses of Cbi-Ex4 and Ex4 on glucoregulation during a standard and a delayed IPGTT

In shrews (n = 14) a standard IPGTT was performed as described above. In this experiment each shrew received IP injection of Ex4 (5 nmol/kg), Cbi-Ex4 (5 nmol/kg) or vehicle in a within-subject, counter-balanced design. Each treatment was separated by 72h.

For the delayed glucose load IPGTT, food (6h pre-IPGTT) and water (4h prior to testing) were removed in a separate cohort of animals (n = 13). A baseline BG reading (t = −360 min) was performed immediately followed by an IP injection of Ex4 (5 nmol/kg), Cbi-Ex4 (5 nmol/kg) or vehicle. BG was measured 3h (t = −120 min), 5.30h (t = −30 min) and 6h (t = 0 min) later and each shrew received IP injection of glucose (2 g/kg). Subsequent BG readings were taken at 20, 40, 60 and 120 min after glucose injection. After the final BG reading, food and water were returned. Each IPGTT round was 72h apart.

Dose-response effects of Ex4 and Cbi-Ex4 on energy balance

We first evaluated in two separate group of shrews the effects on food intake and body weight of different doses of native Ex4 and Cbi-Ex4; respectively. Food was removed one hour prior to dark onset. Shortly before dark onset the first group of shrews (n = 9) received IP injection of Ex4 (1.25, 5 or 50 nmol/kg), or vehicle. In a second group of shrews (n = 10), IP injections of Cbi-Ex4 (1.25, 5 or 50 nmol/kg) or vehicle were performed. Shrews had *ad libitum* access to powdered food through a circular (3 cm diameter) hole in the cage. Food intake was evaluated using our custom-made feedometers, consisting of a standard plexiglass rodent housing cage (29 × 19 × 12.7 cm) with mounted food hoppers resting on a plexiglass cup (to account for spillage). Food intake was manually measured at 6, 24 and 48h post injection. Body weight was taken at 0, 24 and 48h. Treatments occurred in a within-subject, counter-balanced design and were 7 days apart.

Direct comparison of pharmacological doses of Cbi-Ex4 and Ex4 on energy balance

We then compare the effects of Ex4 (5 nmol/kg), Cbi-Ex4 (5 nmol/kg) or vehicle in the same animals (n = 8) using in a within-subject, counter-balanced design. Food was removed one hour prior to dark onset. In this experiment, food intake was evaluated using our custom-made automated feedometers, in which the food hoppers were attached to a load-cell. The amount of powdered food

consumed was measured every 10 s to the nearest 0.1 g (Arduino 1.8.8). Data obtained from the feedometer were processed and converted by computer software (Processing 3.4 and Microsoft Excel) to determine food ingestion every 10 s. Total food intake curves were cumulated for 3, 6 and 24h. Latency to eat (defined as time required before the onset of a meal exceeding 0.25 g) was also measured and analyzed. Treatments occurred 72h apart.

Emetogenic properties of Ex4 and Cbi-Ex4

Shrews (n = 14) were habituated to IP injections and to clear plastic observation chambers (23.5 × 15.25 × 17.8 cm) for two consecutive days prior to experimentation. The animals were injected IP with Ex4 (1.25, 5 or 50 nmol/kg), or vehicle, then video-recorded (Vixia HF-R62, Canon) for 120 minutes. After 120 min, the animals were returned to their cages. In a second group of shrews (n = 14), IP injections of Cbi-Ex4 (1.25, 5 or 50 nmol/kg) or vehicle were performed. Treatments were separated by 7 days. Analysis of emetic episodes were measured by an observer blinded to treatment groups. Emetic episodes were characterized by strong rhythmic abdominal contractions associated with either oral expulsion from the gastrointestinal tract (i.e., vomiting) or without the passage of materials (i.e., retching). Latency to the first emetic episode, total number of emetic episodes and number of emetic episodes per minute were quantified.

Direct comparison of pharmacological doses of Cbi-Ex4 and Ex4 on emesis

Shrews (n = 8) were habituated to the experimental conditions as described above. The animals were injected IP with Ex4 (5 nmol/kg), Cbi-Ex4 (5 nmol/kg) or vehicle, then video-recorded (Vixia HF-R62, Canon) for 120 minutes. After 120 min, the animals were returned to their cages. Treatments were separated by 72 h. Analysis of emetic episodes were measured by an observer blinded to treatment groups. Emetic episodes as well as emetic bouts (defined as series of one or more emetic episodes that occurred within one minute from each other) were evaluated. Latency to the first emetic episode, total number of emetic episodes, number of emetic episodes per minute and total emetic bouts were also quantified.

Assessment of neuronal activation in the DVC following Ex4, Cbi-Ex4 or saline treatments

Body weight-matched shrews (n = 13) received IP injection of Ex4 (5 nmol/kg, n = 3), Cbi-Ex4 (5 nmol/kg, n = 6) or vehicle (n = 4) just prior to dark onset. Food was removed to avoid feeding-related changes in c-Fos expression between groups. Three hours later, shrews were deeply anesthetized with IP triple cocktail of ketamine, xylazine and acepromazine (180 mg/kg, 5.4 mg/kg and 1.28 mg/kg; respectively) and transcardially perfused with 0.1M PBS (Boston Bioproducts), followed by 4% PFA (in 0.1M PBS, pH 7.4, Boston Bioproducts). Brains were removed and post fixed in 4% PFA for 48h and then stored in 25% sucrose for two days. Brains were subsequently frozen in cold hexane and stored at −20°C until further processing. Thirty micrometer-thick frozen coronal sections containing the DVC were cut in a cryomicrotome (CM3050S, Leica Microsystem), collected and stored in cryoprotectant (30% sucrose, 30% ethylene glycol, 1% polyvinyl-pyrrolidone-40, in 0.1M PBS) at −20°C until further processing. IHC was conducted according to previously described procedure (Alhadeff et al., 2015). Briefly, free-floating sections were washed with 0.1M PBS (3x8min), incubated in 0.1M PBS containing 0.3% Triton X-100 (PBST) and 5% normal donkey serum (NDS) for 1h, followed by an overnight incubation with rabbit anti-Fos antibody (1:1000 in PBST; s2250; Cell Signaling,). After washing (3x8min) with 0.1M PBS sections were incubated with the secondary antibody donkey anti-rabbit Alexa Fluor 488 (1:500 in 5% NDS PBST; Jackson Immuno Research Laboratories,) for 2h at room temperature. After final washing (3x8min in 0.1M PBS) the sections were mounted onto glass slides (Superfrost Plus, VWR) and coverslipped with Fluorogel (Electron Microscopy Sciences). c-Fos positive neurons spanning the DVC were visualized (20x; Nikon 80i, NIS Elements AR 3.0) and quantified (FIJI software) using fluorescence microscopy. A total of 4 DVC sections per animal were used to quantify the number of c-Fos labeled cells in the AP and NTS at the level of the obex, caudal medial DVC (200 and 250 μm rostral to the obex, and medial DVC (400 μm rostral to the obex), similarly as previously described (De Jonghe and Horn, 2009) by an experimenter blinded to the treatment.

Emetogenic properties of albiglutide

Shrews (n = 15) were habituated to the experimental conditions (see above). The animals were injected IP with albiglutide (0.5 or 5 mg/kg) or vehicle, and video-recorded for 120 minutes. Treatments were carried out in a within-subject, counter-balanced design and separated by 7 days. Latency to the first emetic episode, total number of emetic episodes, number of emetic episodes per minute and total emetic bouts were quantified.

Effects of albiglutide on energy balance

The effects of albiglutide on food intake and body weight were analyzed similarly as described above. Shrews (n = 10) were injected with albiglutide (0.5 or 5 mg/kg) or vehicle. Food intake was measured manually at 6, 24 and 48h post injection. Body weight was taken at 0, 24, 48, and 72h. Treatments occurred in a within-subject, counter-balanced design and were 7 days apart.

QUANTIFICATION AND STATISTICAL ANALYSIS

All data were expressed as mean ± SEM. For behavioral studies, data were analyzed by a repeated-measures One-Way ANOVA or Two-Way ANOVA, followed by Tukey's post hoc test. For all statistical tests, a p value less than 0.05 was considered significant.

Information on replicates and significance is reported in the figure legends. In the pharmacokinetic study, area under curves (AUCs) were calculated from −10 to 360 or 1440 min using the trapezoidal method, and analyzed using One-Way ANOVA followed by Tukey's post hoc test. BG levels were analyzed using Repeated-measurements Two-Way ANOVA followed by Tukey's post hoc test. AUCs were calculated from 0 to 60 and 0 to 120 min; respectively, using the trapezoidal method. Resulting AUCs were analyzed using Repeated-measurements One-Way ANOVA followed by Tukey's post hoc test. Total number of emetic episodes and emetic bouts were analyzed using Repeated-measurements One-Way ANOVA followed by Tukey's post hoc test. Student's t test was used to analyzed emetic episodes between two equimolar doses. Comparisons between different proportions of shrews experiencing emesis under the different treatment conditions (i.e., occurrence) were made using the Fisher's exact test. Data obtained from the feedometer were analyzed with Repeated-measurements One-Way ANOVA followed by Tukey's post hoc test. For IHC, statistical comparisons were performed using One-way ANOVA followed by Tukey's post hoc test. All data were analyzed using Prism GraphPad 8.

Cell Reports, Volume *31*

Supplemental Information

Corrination of a GLP-1 Receptor Agonist for Glycemic Control without Emesis

Tito Borner, Jayme L. Workinger, Ian C. Tinsley, Samantha M. Fortin, Lauren M. Stein, Oleg G. Chepurny, George G. Holz, Aleksandra J. Wierzba, Dorota Gryko, Ebba Nexø, Evan D. Shaulson, Ankur Bamezai, Valentina A. Rodriguez Da Silva, Bart C. De Jonghe, Matthew R. Hayes, and Robert P. Doyle

Supplementary Figure 1:

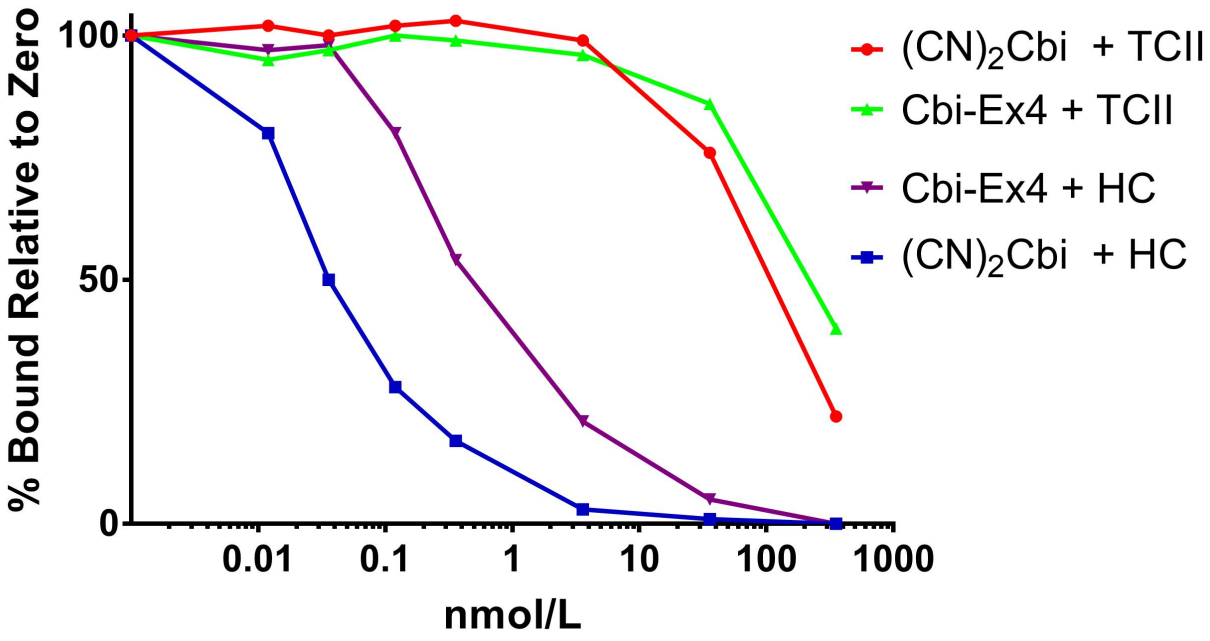

Supplementary Figure S1 (related to Figure 1): Binding affinity plots of Cbi (dicyanocobinamide; $(CN)_2$Cbi) and Cbi-Ex4 by the B12 binding proteins Transcobalamin (TCII) and Haptocorrin (HC).

Figure S1 shows the binding affinity (Ka) of B12 binding proteins transcobalamin and haptocorrin to endogenously occurring Cbi and the Cbi conjugated Ex4 (Cbi-Ex4). HC is known to be the only physiologically relevant binder of Cbi and this is reflected in the binding constant of HC with Cbi (Ka 0.036 nM). HC also binds Cbi-Ex4 (Ka 0.456), albeit with ~ 10-fold lower affinity. Consistent with the known binding profile of TC, only weak binding occurs for TC with Cbi or Cbi-Ex4 (Ka > 2 μM).

Supplementary Figure 2:

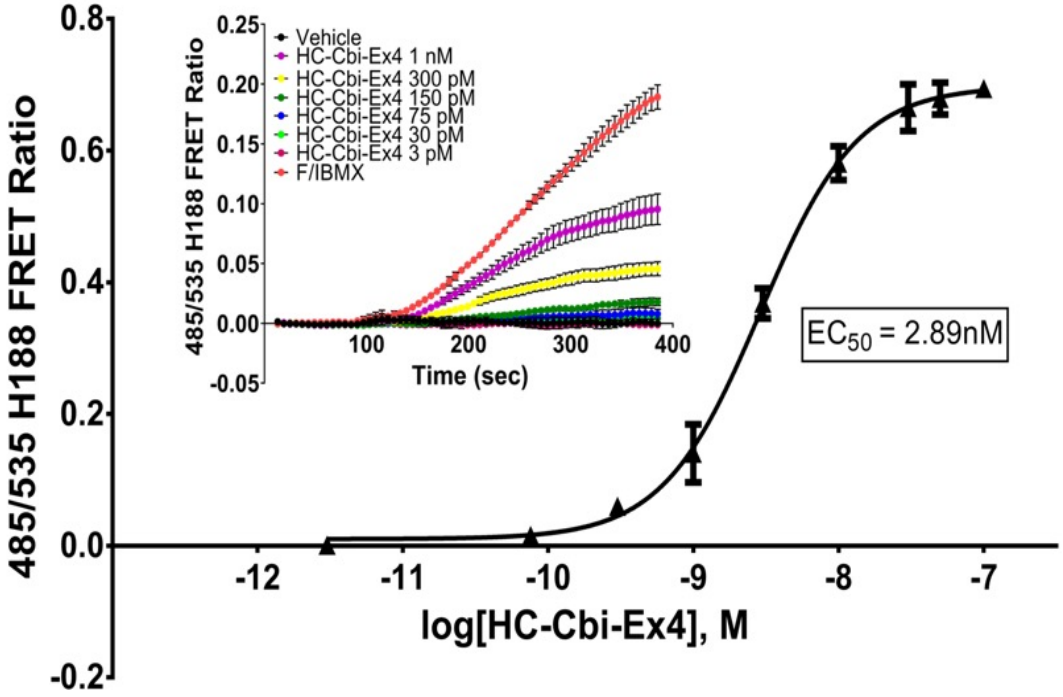

Supplementary Figure S2 (related to Figure 1): Dose response and regression plot for HC-Cbi-Ex4 agonism at the GLP1-R.

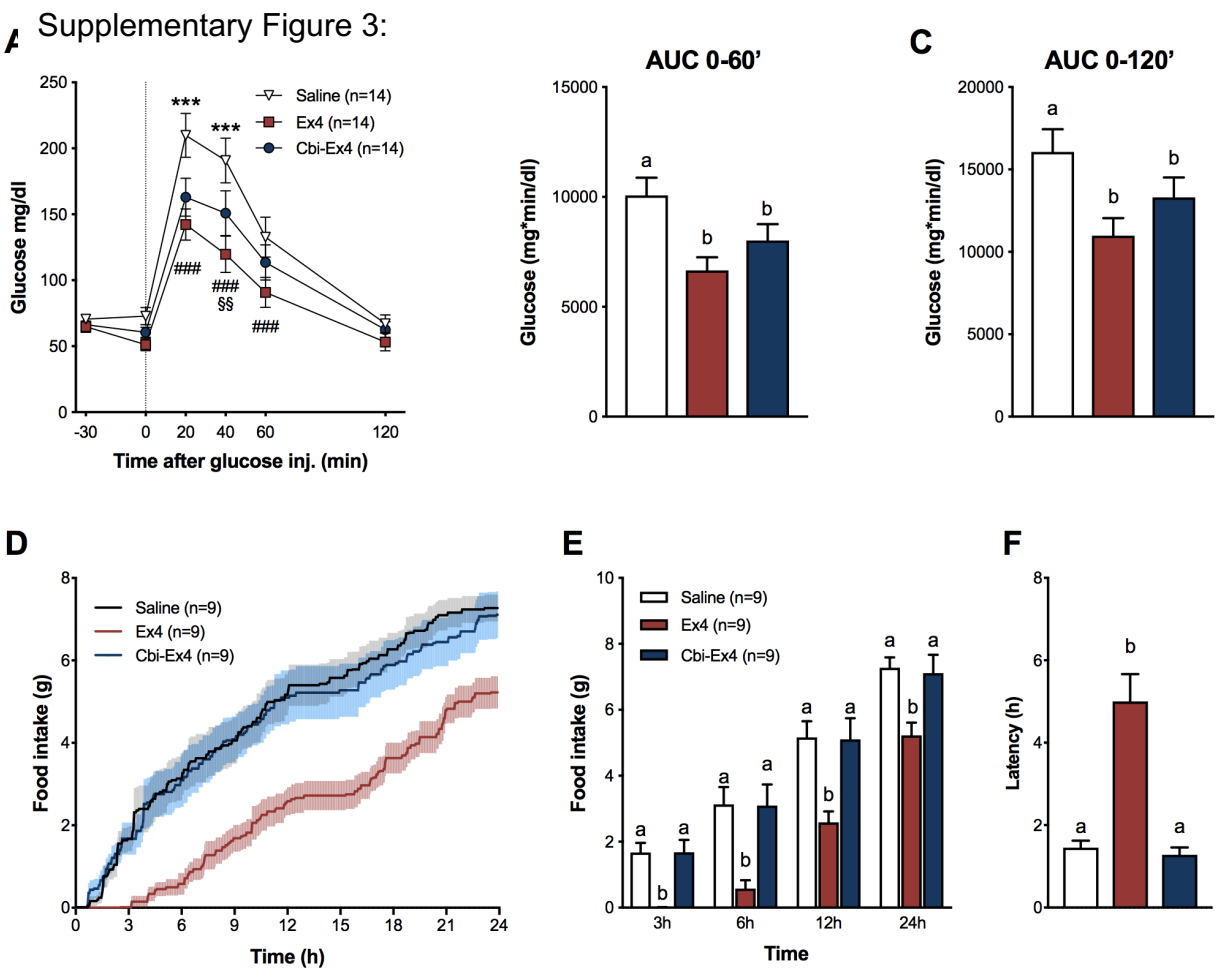

Supplementary Figure 3 (related to Figure 2): Cbi-Ex4 vs. Ex4 direct comparison on glucose clearance and feeding behavior.

A) In an IPGTT, Ex4 (5 nmol/kg, i.e. 20 µg/kg) and equimolar doses of Cbi-Ex4 suppressed blood glucose (BG) levels after IP glucose administration (2 g/kg, IP) compared to saline; vehicle vs Cbi-Ex4: *** $P < 0.001$; vehicle vs Ex4: ### $P < 0.001$; Ex4 vs Cbi-Ex4: §§ $P < 0.01$). **B-C)** Area under the curve (AUC) analyses from 0 (i.e., post-glucose bolus) to 60 and 0 to 120 min; respectively. Cbi-Ex4 and Ex4 similarly reduced AUCs compared to vehicle. **D-E)** Ex4 (5 nmol/kg) induced anorexia at 3h, 6h, 12h and 24h post injection, whereas Cbi-Ex4 had no effect on food intake. **I)** Latency to eat was increased only in Ex4-treated animals. All data expressed as mean ± SEM. Data in **(A)** and **(E)** were analyzed with repeated measurements two-way ANOVA followed by Tukey's post-hoc test. All other data were analyzed with repeated measurements one-way ANOVA followed by Tukey's post hoc test. Means with different letters are significantly different ($P < 0.05$).

Supplementary Figure 4:

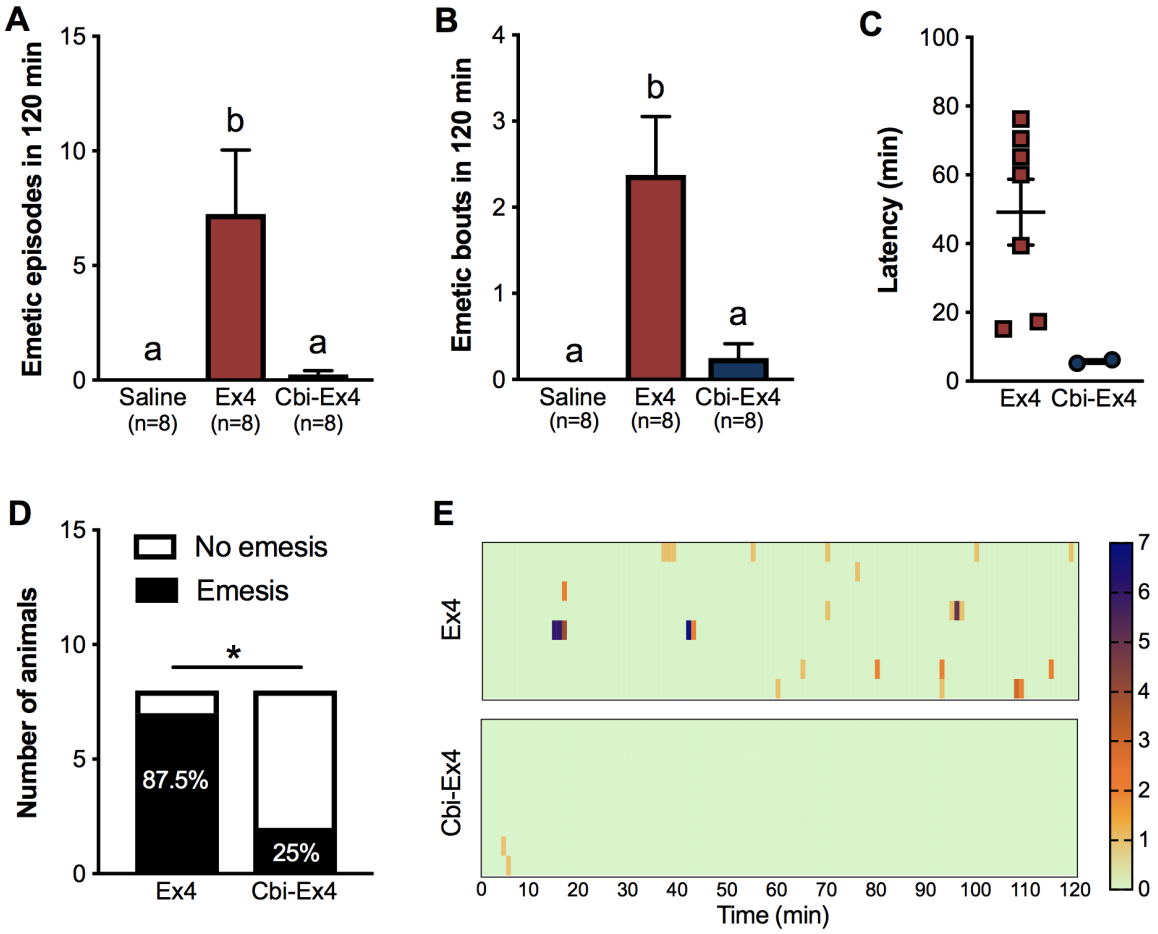

Supplementary Figure 4 (related to Figure 3): Cbi-Ex4 vs. Ex4 direct comparison on emesis.

A) The number of single emetic episodes following, Ex4 (5 nmol/kg, i.e. 20 µg/kg), Cbi-Ex4 or saline administration was recorded for 120 min. Ex4 induced robust emetic responses that were not observed after Cbi-Ex4 or saline injections. **B)** The number of emetic bouts was also lower in Cbi-Ex4-treated animals compared to Ex4 and it did not differ from controls. **C)** Graphical representation of latency to the first emetic episode between Ex4 and Cbi-Ex4-treated animals that exhibited emesis. **D)** The percentage of shrews experiencing emesis was significantly different between Ex4 and Cbi-Ex4. **E)** Heatmap showing latency, number and intensity of emesis for each animal across time. All data expressed as mean ± SEM. Means with different letters are significantly different ($P < 0.05$). Data in **(A,B)** were analyzed with repeated measurements one-way ANOVA followed by Tukey's post hoc test. Data in **(D)** analyzed with Fisher's exact test.

	Shrew Serum	+ Cbi-Ex4, nmol/L, final concentration	
		25	50
Total B12 (nmol/L)	6.51		
B12 Binding capacity (nmol/L)	12.38	6.53	4.74
Apo – TC (nmol/L)	8.04	5.89	4.37
Apo – HC (nmol/L)	4.63	0.640	0.630

Table S1 (related to Figure 1): Vitamin B12 and its binding proteins, Transcobalamin II (TC) and Haptocorrin (HC) as measured in shrew serum, and their inhibition by increasing concentration of Cbi-Ex4.

The sum of Apo TC + Apo HC ~equals B12 binding capacity.

Dose (nmol/kg)	AUC_{0-360} (mg*H/L)	AUC_{0-1440} (mg*H/L)	C_{Max} (nmol/L)	Elimination $T_{1/2}$ (H)	Vd (L)	Cl (L/H)	Ke (H^{-1})
50.0 Ex4	2.82/hr	1.59/hr	32.19 +/- 3.03	14.85	0.12	0.0056	0.047
25.0 Ex4	0.96/hr	0.48/hr	19.80 +/- 2.47	13.52	0.16	0.0082	0.051
50.0 Cbi-Ex4	4.55/hr	2.68/hr	30.96 +/- 2.73	20.48	0.13	0.0044	0.034
25.0 Cbi-Ex4	1.94/hr	1.19/hr	17.25 +/- 1.83	15.99	0.12	0.0052	0.043

Table S2 (related to Figure 1): Pharmacokinetic parameters measured for Ex4 and Cbi-Ex4 in *S. murinus*.
AUC indicates area under the curve between 0 and 360 or 0-1440 minutes; C_{Max} is the maximum measured concentration; $T_{1/2}$ is the elimination half-life; Vd is volume of distribution, Cl is clearance and Ke is elimination rate constant.